European Science Review

№ 5–6 2022

May – June

PREMIER Publishing

Vienna
2022

European Science Review

Scientific journal

№ 5–6 2022 (May – June)

ISSN 2310-5577

Editorial office

Premier Publishing s.r.o. Praha 8 – Karlín, Lyčkovo nám. 508/7, PSČ 18600

E-mail:

pub@ppublishing.org

Homepage

ppublishing.org

European Science Review is an international, German/English/Russian language, peer-reviewed journal. It is published bimonthly with circulation of 1000 copies.

The decisive criterion for accepting a manuscript for publication is scientific quality. All research articles published in this journal have undergone a rigorous peer review. Based on initial screening by the editors, each paper is anonymized and reviewed by at least two anonymous referees. Recommending the articles for publishing, the revЫiewers confirm that in their opinion the submitted article contains important or new scientific results.

Premier Publishing s.r.o. is not responsible for the stylistic content of the article. The responsibility for the stylistic content lies on an author of an article.

Instructions for authors

Full instructions for manuscript preparation and submission can be found through the Premier Publishing s.r.o. home page at: http://www. ppublishing.org.

Material disclaimer

The opinions expressed in the conference proceedings do not necessarily reflect those of the Premier Publishing s.r.o., the editor, the editorial board, or the organization to which the authors are affiliated.

Premier Publishing s.r.o. is not responsible for the stylistic content of the article. The responsibility for the stylistic content lies on an author of an article.

Included to the open access repositories:

The journal has the GIF impact factor 1.36 for 2018.

Typeset in Berling by Ziegler Buchdruckerei, Linz, Austria.
Printed by Premier Publishing s.r.o., Vienna, Austria on acid-free paper.

Section 1. Materials Science

https://doi.org/10.29013/ESR-22-5.6-3-10

Nadareishvili Malkhaz,
PhD, Tbilisi State University,
E. AndronikashviIi Institute of Physics,
Senior Researcher, Georgia
Kiziria Evgeni,
PhD, Tbilisi State University,
E. AndronikashviIi Institute of Physics,
Senior Researcher, Georgia
Sokhadze Victor,
PhD, Tbilisi State University,
E. AndronikashviIi Institute of Physics,
Senior Researcher, Georgia
Tvauri Genadi,
PhD, Tbilisi State University,
E. AndronikashviIi Institute of Physics,
Senior Researcher, Georgia
Gogichaishvili Shota,
PhD, Tbilisi State University,
E. AndronikashviIi Institute of Physics,
Researcher, Georgia
Jeremy Ramsden,
Professor, University of Buckingham, MK18 1EG, UK

PULSED DIFFERENTIAL CALORIMETRY OF THE HEAT CAPACITY JUMP AT DENATURATION OF COLLAGEN TYPE I OF RAT TAIL TENDONS

Abstract. The estimation of the heat capacity jump at melting of collagen fibers having principle significance for determination of the role of hydrophobic interactions in the process of formation and stabilization of collagen fibers was performed for collagen type I of rat tail tendons in an aqueous medium and in 0.5M acetic acid. The research was performed by using the unique high-precision pulsed differential scanning calorimeter (PDSC) designed by the authors. The device provides a measurement of heat capacity in the pulsed mode under the thermodynamically equilibrium conditions, in contrast to usual differential scanning calorimeters (DSC) performing the measurements in the continuous heating mode. The measurements carried out in the pulsed mode allow the exact determination of heat capacity before and after denaturation transition. The experiments showed that magnitude of the heat capacity jump in the aqueous medium is twice as large as the value of the jump in 0.5M acetic acid. The melting temperature in the aqueous medium was by 22 °C higher than in acetic acid and, the melting enthalpy in the aqueous medium was more too. The obtained results are discussed in the light of the data available in the literature regarding this problem.

Keywords: Collagen fibers melting, Pulsed differential scanning calorimetry (PDSC), Heat capacity jump at denaturation of collagen, Hydrophobic interactions.

Introduction

Collagen is the basic protein of the connective tissue in living organisms. It attends support and protective functions, and plays an important role in the processes of differentiation and growth of the organism, and its adaptation to the environment in the process of evolution. The functional diversity of collagen has determined the interest to its structure and biology among researchers for decades [1–8]. The problem of the formation and temperature stability is among key ones in the biology and physics of collagen. Temperature plays an essential role in the vital activity of biological systems. All catalytic processes proceeding with participation of biological Macromolecules, the temperature coefficient of which is higher than that of low molecular compounds, both in *vivo* and in *vitro* depend on the temperature. Various mechanisms of adaptation to the changes in the environmental temperature resulted in the existence of the variety of living systems and hence in the variety of biological macromolecules functioning optimally only at the physiological body temperature for homeothermic animals and at some optimal temperature for endothermic animals.

There is not observed a direct relation between the degree of the evolution of collagen and the degree the heat stability. Hence it is assumed that the phylogenetic changes in heat stability hold only adaptive significance [9]. Phylogenetic adaptation occurs at the level of the genetic apparatus and involves irreversible profound changes in biological macromolecules [10], unlike season adaptations that are short-term and of a reversible character. The collagen molecule is actually the only bio macromolecule the temperature of denaturation of which strictly follows the physiological body temperature.

The process of collagen biosynthesis results in the formation of collagen fibers, the stability temperature of which exceeds the temperature of denaturation of a triple helix in the solution by 22 °C in average [1]. Though there is some success in understanding the nature of forces responsible for the increase of fibril stability the problem has not been adequately studied yet. Some contribution to the increase of the temperature of fibril melting, as compared to the triple helix, can be made by hydrophobic interactions [2], which, as it is known, are of entropy nature.

As is known from the study of thermodynamic properties of globular proteins, for the estimation of the role of hydrophobic interactions the most efficient approach is the measurement of the heat capacity jump at the transition of protein from native state to the denaturation one [2]. In the same work, the value of the heat capacity jump with the denaturation of rat skin collagen macromolecules was assessed according to circumstantial evidence. As for fibrils there is no evidence even of that kind. Therefore, in this work the effort was made to estimate by direct precision calorimetric measurements the value of the heat capacity jump at melting of the collagen fibers of rat tile tendons in water, where collagen remains as fibrils, and in 0.5 M acetic acid, in which collagen exists as separate triple helixes and has different degrees of stability [1] i.e. different temperatures of denaturation.

A unique pulsed differential scanning calorimeter (PDSC) created by the authors allows performing the measurements of the above-mentioned heat capacity jumps in a pulsed mode under the thermodynamically equilibrium conditions with high precision, in contrast to conventional differential scanning calorimeters (DSC) performing the measurements in the continuous heating mode under not un sufficiently equilibrium conditions. Obtained results are discussed in the light of existing representation on the properties of the triple helix and collagen fibers [11].

Rat tail tendon preparation

Tails of six week-old rats were excised from the carcasses and released from the skeleton. The fibrils were immediately washed in distilled water, and all visible contaminants were removed from the fibrils under the microscope. In order to exclude the side effects connected with the change in the amount of hydrated water and with age-related changes [12], the experiments were carried out on the fibrils from one and the same object. Prior to the experiments, the fibrils were dried in vacuum at room temperature in order to remove the remained moisture. The collagen fibrils cleaned in this way contain of 97% of pure collagen [12]. The fibril in amount of 10–20 mg was placed into a calorimetric cell, the distilled water or 0.5 M acetic acid was added and kept for a night before starting the experiment. Another cell of the differential calorimeter contained the same amount of distilled water or 0.5 M acetic acid respectively.

Calorimeter

The measurements of a heat capacity jump at melting of collagen fibers were carried out with the help of the unique, high sensitive and precise pulsed differential scanning calorimeter (PDSC) based on the original method elaborated by the authors [13–17].

At present the most sensitive calorimeters are differential scanning calorimeters (DSC) [18–20], including temperature modulated DSCs (TM DSC) [21], but DSCs have one important disadvantage: they measure heat capacities difference between sample and standard at not strongly equilibrium conditions. The reason is that in continuous heating mode, to both cells of differential container continuously is served the same power P, because of the difference in the heat capacities of the sample and standard $\Delta C = C_2 - C_1$ they are heated unequally, but soon there comes a stationary mode when cells are heated at the same rate $\frac{dT}{dt}$, due to the transition from one cell to another heat power $P = k\Delta T$, by the thermobattery between the sells, where k is the thermal conductivity of the thermobattery, and ΔT – the temperature difference between the cells. From the simple thermodynamic calculations follow, that in a stationary mode

$$\Delta T = \left(\frac{1}{2K}\right)\cdot \Delta C \cdot \left(\frac{dT}{dt}\right) \quad (1)$$

As can be seen, the temperature difference between the cells and therefore the value of the emf of the thermobattery between the cells (signal) depends not only the value of the heat capacity difference between the cells, but the heating rate too. The higher is the heating rate, the higher is the signal. Hence, for observation small thermal effects, when the emf of thermobattery is very small, one can increase the signal and make it measurable using high speeds of heating. However, at high heating rates, temperature gradients develop in the samples and the measurements are performed under non-equilibrium conditions, because of it the registered heat capacity difference DC(T) may differ from its true value, depending on the heating rate. About similar effect was mentioned in work [22].

The above – mentioned incompatibility of high heating rates with the adequacy of measurements limits the opportunity of measuring small heat capacity differences and the accuracy of the measurement conventional differential scanning calorimeters.

PDSC allows combine high heating rates with accurate measurements. This is achieved by using the method of pulsed heating with temperature scanning. Due to the high rate of heating during the short but powerful impulse in the pulsed mode signal is much higher with compared the continuous heating mode, at the same time the measurements were carried out in the equilibrium conditions, since at the beginning and after the end of a short pulse sample is in thermal equilibrium conditions and the heat effect under study remains undistorted [16]. Thus, using PDSC one can measure small deviation of heat capacity with high accuracy or observe such small effects, which in studies using conventional DSC can be just as well stay undetected. Therefore, PDSC exactly suitable for the task assigned in this article: precise measuring of the small jump of the heat capacity at the denaturation of collagen.

The relative error of measurements is $\delta C/C \approx 10^{-4}$, where δC is the error of measurements and C is the absolute heat capacity of the cell.

Calorimeter capable to work in a continuous heating mode too, similar to a conventional continuous heating DSCs. The rate of scanning at the continuous heating is possible to change from 6 K/h to 60 K/h.

The described calorimeter is also effective for the study of isothermal processes with high accuracy.

Experiment

The measurements of the heat capacity jump of collagen fibers at melting were made under two different conditions: in acetic acid and in water. In one of the cells of calorimetric container 20 mg of dried fiber was placed and 0.95g distilled water or 0.5 M acetic acid added. In other cell the same amount of water or 0.5 M acetic acid was poured respectively. The amount of water was controlled by analytical scales. In order to eliminate the additional errors connected with age-related changes and with other factors, all experiments were carried out on the fibrils of one and the same object.

The estimation of size of thermal capacity jump at the melting of collagen, is not a simple task, because of many factors influencing on size of this jump. Besides the above factors it is necessary to allocate kinetic character of melting of collagen which can influence this size [22]. Therefore, to exclude this artefact it is necessary to lead measurement in equilibrium conditions that was achieved in this work.

Figure 1 shows the results of investigation of denaturation of collagen in aqueous medium and in 0.5 M acetic acid. The measurements were performed in continuous heating mode at the speed of 15K/hour. It is seen that the heat absorption peaks are shifted acros the temperature by the expected value: 22 °C and are of different shape. Phase transition enthalpy calculated from these graphs is $\Delta H = 50.2\ \mathrm{Jg}^{-1}$ in 0.5 M acetic acid and $\Delta H = 60.1\ \mathrm{Jg}^{-1}$ in water respectively.

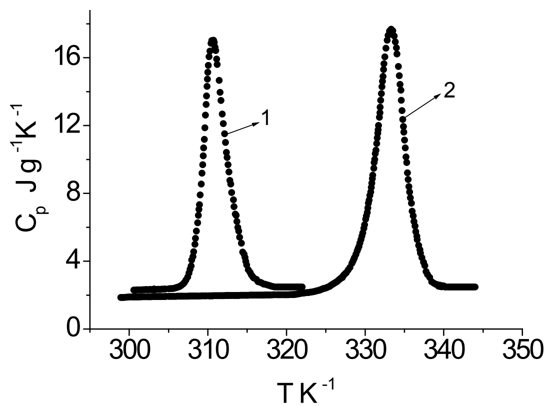

Figure 1.

Calorimetric curves of melting of collagen fibers in 0.5M acetic acid (curve 1) and water (curve 2).

Calculation the enthalpy of denaturation $\Delta H(T_d)$ occurred by numerical integration of the expression

$$\Delta H(T_d) = \int_{T_1}^{T_2} C(T)dT \qquad (2)$$

Where T_1 and T_2 are the temperature of the beginning and ending of the denaturation process, T_d is the denaturation temperature, $C(T)$ is the "heat capacity" of the collagen during the melting (Figure 1), $C(T)\,dT = dH(T)$ is the adsorbed heat as the temperature increases on dT – elementary area between the transition curve and the baseline. For one transition curve two basic lines are drawn: one – on the experimental points before the beginning of the transition process, below T_1, by extrapolation of which to T_d, the basic line for the temperature interval $T_1 - T_d$ was obtained and the second – on the experimental points after the end of the transition process, above T_2, by extrapolation of which to T_d, the basic line for the temperature interval $T_d - T_2$ was obtained

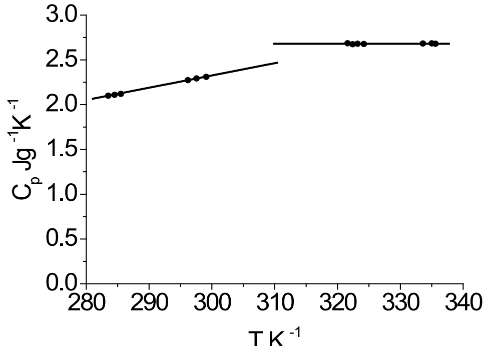

Figure 2. Heat capacity jump at melting of collagen in 0.5M acetic acid

0.5M acetic acid and in water are: ΔC_p=0.2 $Jg^{-1}K^{1}$ and ΔC_p=0.46 $Jg^{-1}K^{-1}$ respectively.

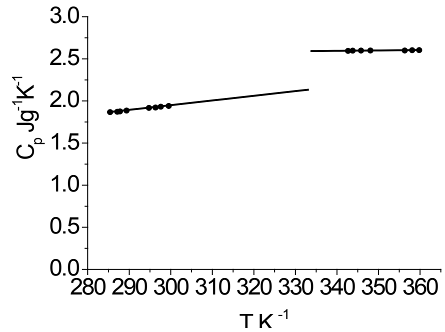

Figure 3. Heat capacity jump at melting of collagen in water

Figure 2 and Figure 3 present the temperature dependencies of collagen heat capacity in acetic acid and in water. Prior to transition, the heat capacity of collagen in acetic acid is higher than in water. The temperature coefficient of heat capacity in acetic acid is three times higher than that in water. Heat capacity jump at the denaturation in

After denaturation, the heat capacity of collagen in acetic acid and in water sligthly depend on temperature and is equal to ~ 2.62 $Jg^{-1}K^{-1}$.

In table are given the results of measurements some thermodynamic characteristics of rat tail tendon collagen obtained by calorimetric measurements in water and 0.5 M CH_3COOH.

Table 1.

Environment	**Denaturation temperature °C**	**Denaturation Enthalpy $\Delta H_r(T_d)$ Jg^{-1}**	**Heat Capacity Jump $\Delta C_p(T_d)$ $Jg^{-1}K^{-1}$**
Water	63 +/–0.2	60.1 +/–0.3	0.46 +/–0.02
0.5M Acetic acid	40.8 +/–0.2	50.2 +/–0.3	0.20 +/–0.02

Discussion

Acid solutable collagen exists in the form of a triple helix in the pH interval from pH = 2.0 to Ph = 4.0, which can be represented approximately in the form of elongated sticks. The researchers estimated the average molecular parameters of collagen macromolecules by different methods such as light scattering [23], statistical processing of electron-microscopic data [24], double refraction and viscosity [25]. The obtained average results were as follows: length 2800 A°, diameter 15 A°, molecular weight – 30000d. It should be noted that, in the interval of pH 2.0–4.0, the temperature of denaturation of collagen depends only slightly on the pH value. In water collagen exists as fibrils.

As it was mentioned above the problem of stabilization of collagen structure is one of the leading problems in physics and biology of collagen due to its functional importance connected with the phylogenetic change of thermal stability in the process of evolution [26; 27]. The main component of connective tissue – triple helix of collagen should be rather flexible on the one hand, in order to be able to form the fibrils spontaneously outside the cell under the physiological conditions, and, on the other hand, it should provide the formation of stable connective tissue capable to serve as mechanical functions. Both these properties are revealed in low temperature of denaturation of triple helix (T_d) in solutions within pH-2–4 interval, and in the increase of the temperature of shrinkage of collagen fibers (T_s) [28].

The important role in formation of collagen fibers and growth of melting temperature *in vivo* together with other factors can play hydrophobic interactions the presence of which can be fixed and estimated by size of thermal capacity jump at the melting of collagen fibrils [2].

The difference between the temperatures of collagen fibers melting and denaturation of triple helix in the solution of different origin remains constant: 22 °C in average, as it was pointed above. Coiling into triple helix is achieved by intramolecular hydrogen bonds connecting the HN group of the glycine residue on one chain to a C=O group on an adjacent chain in the first position of collagen triplet $(Gly\text{-}X\text{-}Y)_n$ [29] by water molecules in the second position [30] and by the residues of hydroxyproline in the third position of triplet [31]. The further arrangement of collagen fibers in tissue takes place as a result of the change of surface charge of triplet helix, or by hydrophobic interactions between side-groups of amino acids [32; 33].

At present, the fundamental dependence of the enthalpy denaturation of collagen on the content of hydroxyproline and a slight change of enthalpy from 57.5Jg^{-1} to 58.2Jg^{-1} at the change of pH in 2–4 interval for the collagen of rat skin are determined[27]. This allowed one to predict the approximate value of heat capacity jump: 20 $Jmol^{-1}K^{-1}$ in the mentioned pH interval [2]. Hydrophobic interactions between the side groups of amino acids in the triple helix that can contact with each other, could be revealed by direct measuring of heat capacity jump at melting. According to our direct measurements the value of heat capacity jump for collagen of rat tile in 0.5 M acetic acid makes 0.2 $Jg^{-1}K^{-1}$, in agreement with above prediction, but the jump at denaturation of collagen fibers in the aqueous medium (0.46 $Jg^{-1}K^{-1}$) is twice and even more times bigger. A preliminary report about the existence of the specific heat jump of fibrils in water was made in [34]. The difference in the values of heat capacities jumps in water and in acetic acid may be explain by different nature of interactions of side chains of amino acid. It may be hydrophobic interactions nature, as in the literature there are data indicating the role of hydrophobic interactions at the **formation** of collagen fibers in mediums containing CH-groups with different degree of polymerization [30]. If we compare the results obtained by us with the results obtained for the heat capacity jumps in globular proteins, in which the hydrophobic interactions really determine the stability of globule, its value in collagen is of the same order, as in ribonuclease – the protein with the lowest level of hydrophobic interactions [35]. The relation between the value of heat capacity jump and the hydrophobic interactions is followed unambiguously on the example of globular proteins. For the majority of globular proteins, the hydrophobic interactions play the important role for the stability of globule in polar solvents. Such peculiarity of globular proteins is seen well in inversely proportional dependence of the enthalpy of collagen denaturation on the value of heat capacity jump [36; 37].

The facts, determined by us consisting in that both the enthalpy and heat capacity jump at melting of fiber in water are higher than that at melting of collagen in the solution of acetic acid make basis for the assumption that the hydrophobic interactions do not play such remarkable role in the increase of melting temperature, as it was in the case of globular proteins [35; 36]. Logically it seems more reasonable to assume that in the increase of the temperature of melting, the more important role can have the electrostatic interactions between the side-groups of amino acids, though the definite value of jump does not exclude the role of hydrophobic interactions. The obtained results give the definite idea about the physical-chemical nature of formation of collagen fibrils, but of course, the further investigations are needed to show the real process of fibril genesis.

Conclusions

1. By using the high precision pulsed differential scanning calorimeter (PDSC) the jumps of heat ca-

pacity at melting of collagen fibers of rat tails tendons in water and in 0.5M acetic acid were measured under the thermodinamically equilibrium conditions.

2. It is shown that the jumps of heat capacity of rat tail tendons collagen in water are twice as large as in 0.5M acetic acid.

3. The enthalpy of denaturation of rat tail tendons collagen in water is more than in acetic acid too.

4. The obtained results are discussed in the light of existing idea about the mechanism of fibril formation.

5. On the basis of the increase both enthalpy and the heat capacity jump at the melting of collagen of rat tail tendons in aqueous medium, as compared to the enthalpy and the heat capacity jump at denaturation in acetic acid, it is assumed that in the process of formation of these collagen fibrils the participation of electrostatic interactions of side groups of amino acids is probably more important than the participation of hydrophobic interactions.

References:

1. Rigby B. J., J. Thermal Biology,– 2. 1977.– P. 89–93.
2. Privalov P. L. Adv. Prot. Chem,– 35. 1982.– P. 1–104.
3. Tao Qu, Vikas Tomar, International Journal of Experimental and Computentional Biomechanics,– Vol. 3. 2015.– Iss. 1.– P. 62–81.
4. Tao Qu, Vikas Tomar. Materials Science and Engineering: C,– Vol. 38. 2014.– P. 28–38.
5. Perumal S., Antipova O. & Orgel J. P. PNAS – 105 (8). 2008.– P. 2824–2829.
6. Orgel J. P., Irving T. C. PNAS.– 103(24). 2006.– P. 9001–9005.
7. Cacace M. G., Landau E. M. and Ramsden J. J. Quarterly Reviews of Biophysics, Cambridge University Press,– 30, 3. 1997.– P. 241–277.
8. Nadareishvili Malkhaz. European Science Review,– No. 9–10. 2021.– P. 3–6.
9. Nordvig A., Hayduk U., J. Mol. Biol.– V. 44.– No. 1. 1969.– P. 161–172.
10. Aleksandrov V. Ia. Yspexi Sovremennoi Biologii (Rus.) – V. 67.– Iss. 2. 1969.– P. 383–399.
11. Miles C. A., Burjanadze T. V. Biophysical Journal,–80. 2001.– P. 1480–1486.
12. Miles C. A. Ghelashvili M. Biophysical Journal,– 76. 1999.– P. 3243–3252.
13. Basilia G. G., Kharadze G. A., Kvavadze K. A., Nadareishvili M. M., Brewer D. F. Pulsed differential calorimetry of Zn-doped LSCO cuprates, Low Temperature Physics – 24 (8). 1998.– P. 547–550.
14. Nadareishvili M. M., Kvavadze K. A., Basilia G. G., Dvali Sh. A., Khorguashvili Z. Journal of Low Temperature Physics.,– Vol. 130.– Nos 5/6. 2003.– P. 529–542.
15. Nadareishvili M., Kiziria E., Sokhadze V., Tvauri G. The problem of high heating rate in differential calorimetry, European Conference on Innovations in Technical and Natural Sciences, 2017.– P. 149–152.
16. Nadareishvili M., Kiziria E., Sokhadze V., Tvauri G., Tsakadze S. New method of differential calorimetry. European science review, 2017.– P. 253–255.
17. Khoperia T., Zedginidze T., Kvavadze K., Nadareishvili M. Development of competitive nanotechnologies for solution of challenges in photocatalysis, electronics and composites fabrication. 212th Meeting of the Electrochemical Society. Abstract – 107, 2007.
18. Privalov G. P., Kavina V., Freire E. Privalov P. L. Anal. Biochem.,– V. 232. 1995.– P. 79–85.
19. Loram J. W., J. Phys. E: Sc. Instrum.,– Vol. 16. 1983.– P. 367–375.
20. Hohne G. W. H., Hemminger W. F., Flammersheim H.-J.– Differential Scanning Calorimetry, springer-verlag – Berlin, 2003.– 195 p.

21. Modulated temperature differential scanning calorimetry: theoretical and practical applications in polimer characterization, Edited by Mike Reading, Douglas J. Hourston, Dordrecht, The Netherlands. 2006.– 328 p.
22. Christopher A. Miles, Thengiz V. Burjanadze and Allen J. Bailey, J. Mol. Biol.,– 245. 1995.– P. 437–446.
23. Boedtker H., Doty P., J. Amer. Chem. Soc.,– V. 78.– No. 17. 1956.– P. 4267–4280.
24. HaLL C.E., Doty P. A., Amer. Chem. Soc.,– V. 80.– No. 4. 1958.– P. 1269–1274.
25. Rice R. V., Casassa E. F., Kerwin R. E., Maser M. D., Arch. Bioch. Bioph,– V. 105.– No. 3. 1964.– P. 409–423.
26. Burjanadze T. V. Biopolymers – 21. 1982.– P. 1489–1501.
27. Burjanadze T. V. Biopolymers – 32. 1992.– P. 941–945.
28. Burjanadze T. V. Evidence for the role of 4-hidroxiproline in adaptation changes of thermostability of a collagen molecule and collagen Fibrils, Biopolymers,– V. 21. 1982.– P. 1489–1501.
29. Riich A. Crick F. H.C., J. Mol. Biol.,– 3. 1961.– P. 483–506.
30. Ramachandran G. N., Chandrasecharan R. Biopolymers – 6, 11. 1968.– P. 1649–1661.
31. Ramachandran G. N. Bansal M. and Bhatnagar R. S. Bioch. Biophys. Acta.,– 322. 1973.– P. 166–171.
32. Tiktopulo E. I. Kajava A, V. Biochemistry – 37. 1998.– P. 8147–8152.
33. Schnell J. Arch.Bioch. Biophys.,– 127. 1968.– P. 496–502.
34. Nadareishvili M., Burjanadze T., Kvavadze K., Kiziria E., Gelagutashvili E.– Arxiv: 1206.3908.
35. Privalov P. L. Edv. Protein Chem.,– 33. 1979.– P. 167–241.
36. Burjanadze T. V., Tiktopulo E. I., Privalov P. L. Dokladi Academii Nauk (Russian),–V. 293. 1987.– P. 720–724.
37. Burjanadze T. V., Veis A. Connective tissue research,– 36. 1997.– P. 347–365.

Section 2. Medical science

https://doi.org/10.29013/ESR-22-5.6-11-15

Jiemuratova Gulparshin Koshkinbayevna,
Candidate of Medical Sciences,
Senior Researcher at the Nukus branch of the Institute of Human Immunology and Genomics of the Academy of Sciences of the Republic of Uzbekistan, Nukus, Uzbekistan

Kalandarova Amina Nurullayevna,
MD, Head. laboratory of the Nukus branch of the Institute of Human Immunology and Genomics of the Academy of Sciences of the Republic of Uzbekistan, Nukus, Uzbekistan

Kadyrova Aigul Amirbekovna,
Junior Researcher of the Nukus branch of the Institute of Human Immunology and Genomics of the Academy of Sciences of Uzbekistan, Nukus, Uzbekistan

THE INFLUENCE OF ENVIRONMENTAL FACTORS ON THE NONSPECIFIC IMMUNITY OF CHILDREN LIVING IN THE ARAL SEA REGION

Abstract

Objectives. A man in the Aral Sea region found himself under the influence of a complex of habitat factors, in close dependence on the quantity and quality of the available water resources of which, acting through nonspecific and specific immunity factors, can cause profound changes in the human body.

Aims. Assessment of the state of the immune system and the elemental status of children, taking into account the water factor in the ecologically unfavorable region of the Aral Sea region.

Materials and Methods: A comprehensive study of the quality of various categories of drinking water (tap, well, open water bodies) by the most important physical and chemical components was carried out: water salinity (dry residue), hardness (Ca + Mg), chloride and sulfate content, pH, the presence of organic matter (according to BOD5 and permanganate oxidizability), biogenic elements, macro-and microelements, and assessment of the state of the immune system and elemental status in 150 healthy children born and permanently residing in the Aral Sea region.

Results: A correlation was established between the quality of drinking water and the morbidity of children with the concentration of sulfates in water r = 0.83, chlorides in water r = 0.52, hardness (r = 0.40), and salinity (r = 0.53) drinking water. Assessment of adaptive reactions according to the leukocyte formula of a general blood test revealed an increased activation of the body's adaptive system. The relationship between the influence of environmental factors and the incidence of children in the Aral Sea region was revealed.

Conclusions. The water factor in the Aral Sea region is one of the dominant factors in the occurrence of various pathological conditions in children. In the Aral Sea region, children develop violations of the macro-and microelement status, the immune system, which under normal conditions are mobile, have a pronounced margin of safety and the information content of which is especially high.

A decrease in the quality of drinking water affects the hemogram, increasing the content of leukocytes, as well as the relative and absolute content of lymphocytes, reducing the relative and absolute content of monocytes. These changes, depending on the place of residence, are explained by the reaction of the immune system to the influence of environmental pollution.

Keywords: environmental factors, macro-and microelements, the Aral Sea region, adaptive response, morbidity in children.

Introduction

The human body in the process of life is exposed to a complex of environmental factors of polytropic action, which contribute to the formation of altered reactivity of the body, increasing the risk of developing various diseases [9]. The quality of the environment largely determines the level of the human body's defenses [1]. A man in the Aral Sea region was under the influence of a complex of habitat factors, many of which, acting through nonspecific and specific immunity factors, can cause profound changes in the human body [2].

Adaptation of the body to constantly changing environmental conditions (external and internal) is a continuously occurring process designed to maintain homeostatic balance in the body. The adaptive capabilities of the organism are increasingly considered as one of the important criteria of health since the modern understanding of the disease includes the idea of defense mechanisms, first of all, the mechanisms of adaptation and compensation [3].

Physiological mechanisms of adaptive restructuring of the child's body in ecologically unfavorable conditions naturally lead to shifts in elemental homeostasis [2]. The human habitat and the state of his health in the Aral Sea region turned out to be closely dependent on the quantity and quality of available water resources. With water, a person receives 1–25% of the daily requirement for physiologically necessary chemicals [4]. Mineral substances that enter the human body with water have a more significant physiological value than those that come with food since the latter lose some of their amount in the process of cooking [5]. It is necessary to study the direction of changes in the nonspecific immunity of children, depending on the area of residence, to find and justify ways to correct changes in the immune status in order to improve the quality of life of the population in ecologically unfavorable regions [6].

Aims. Assessment of the type of nonspecific adaptive reactions of the body and the elemental status of children, taking into account the water factor in the ecologically unfavorable region of the Aral Sea region.

Materials and Methods

In the city of Nukus, the Republic of Karakalpakstan, using atomic absorption spectrophotometry, a comprehensive assessment of tap drinking water was carried out for the most important physicochemical components: water salinity (dry residue), hardness (Ca + Mg), chloride and sulfate content, pH, the presence of organic matter (BOD5 and permanganate oxidizability), biogenic elements, macro-and microelements. A comparative assessment of indicators of macro-and microelements in drinking water and blood serum of children was carried out, as well as an assessment of the type of nonspecific adaptive reactions according to the leukocyte formula of a general blood test (the number of leukocytes, the relative and absolute content of lymphocytes and monocytes) in 150 healthy children born and permanently residing in the region Aral Sea.

Results

In the selected samples of drinking water there are suspended solids or coarse impurities. According to the requirements for the composition and properties of water, the content of suspended solids as a result of the discharge of wastewater should not increase by more than 0.25 and 0.75 mg/l. In accordance with the hygienic requirements for the quality of drinking water, the turbidity should not exceed 1.5 mg/l [4]. In the investigated drinking water of the regions, the turbidity is 5–29 mg/l.

The salinity of drinking water is subject to drastic changes. In all the water samples we have taken, the mineralization exceeds the MPC by 0.36–0.83 times.

Substances in drinking water in low concentrations, but playing an important role in many physiological processes, are of great importance [5]. A study of the composition of macro-and microelements in water samples revealed their mosaic distribution.

The concentration of Co in the well water of the Muynak region is 2 times higher than the MPC, 1.6 times in the Kungrad region, and 4 times in the Kanlykul region. It is known that excess Co in drinking water causes chronic intoxication, characterized by diseases of the upper respiratory tract, allergic symptoms, bronchial asthma, and allergic dermatoses, as well as the so-called "cobalt cardiomyopathy" [8]. The Fe content in all the samples taken was below the MPC level. Fe deficiency in children can lead to increased absorption of Co in the digestive tract.

The content of Zn in the drinking water of the study areas was almost 500 times lower than the MPC. Zn deficiency conditions are usually characterized by the presence of symptoms such as decreased appetite, anemia, allergic diseases, dermatitis. T-cell immunity is specifically reduced, so children with Zn deficiency usually often and for a long time suffer from colds and infectious diseases. Upon contact with various chemical factors, the homeostasis of the body is provided by the immune system in conjunction with the neurohumoral regulation system. As a result of anthropogenic hyperchimization of the environment during the transient, and especially with prolonged exposure to the body of agents with immunotoxic and immunomodulatory properties, the risk of developing immunopathological conditions, allergic diseases increases [9].

When examining children, it was revealed that Ca deficiency in blood serum is present in 44%, and Fe in 39%, while in the clinical picture hypochromic anemia, inflammatory changes in mucous membranes, and chronic gastroduodenitis, as well as immunodeficiency states, were more often detected.

The incidence of children is closely correlated with environmental pollution with pesticides ($r = 0.66$), the quality of drinking water (with the concentration of sulfates in water $r = 0.83$ and chlorides in water $r = =0.52$). A correlation was established between the incidence of children and the hardness ($r = 0.40$) and mineralization ($r = 0.53$) of drinking water.

L. H. Garkavi et al. made it possible to identify 4 types of nonspecific adaptive reactions arising from the effects of endogenous and exogenous stimuli of any kind with different strengths and reflecting mainly the combined participation of the immune and endocrine links of adaptation. All reactions that are a nonspecific basis of a pre-illness or illness are classified as stressful reactions. As signal indicators of the body's adaptive response in clinical practice, the authors proposed criteria based on the indicators of the leukocyte formula of the general blood test [3].

The results of the conducted studies showed that the content of leukocytes in children was in the range from 6.75 ± 0.49 to 7.08 ± 0.14, averaging 6.915 ±0.31. By the type of nonspecific adaptive reactions, the deviations of the indicators were within the value for the degree of tension II.

The absolute lymphocyte count in children ranged from 2.79 ± 0.21 to 3.13 ± 0.17, averaging 2.96 ± 0.19. The relative content of blood lymphocytes in children was from 36.52 ± 2.68 to 45.12 ± 1.7, averaging 40.82 ± ± 2.19. The indicators were within the values for the degree of tension IV. This indicates an increased activation of the body's adaptive system, which, according to L. Kh. Garkawi increases the secretion of ACTH and glucocorticoids and determines the different effects of these reactions on inflammation, including a certain ratio of the activity of the blood coagulation and anticoagulant systems, which indicates an increase in the activity of the defense systems the organism of children in response to environmental changes in the Aral Sea region. The health level gradually decreases with increased activation [11].

The absolute content of monocytes was from 0.29 ± 0.03 to 0.31 ± 0.05, averaging 0.3 ± 0.04. The relative content of monocytes in the blood of children was from 3.98 ± 0.43 to 4.28 ± 0.43, averaging 4.13 ± 0.43. The indicators were below the minimum deviation range. Probably, the decrease in the absolute and relative content of monocytes in children permanently residing in the Aral Sea region is due to a large number of pesticides with environmental pollution (r = 0.66), the quality of drinking water (with a concentration of sulfates in water r = 0.83 and chlorides in water r = 0.52) [12].

Assessment of adaptive reactions according to the leukocyte formula of a general blood test revealed an increased activation of the adaptive system of the body of children. The relationship between the influence of environmental factors and the incidence of children in the Aral Sea region was revealed.

Conclusion

Thus, our studies show that the water factor in the Aral Sea region is one of the dominant factors in the occurrence of various pathological conditions in children. Good-quality drinking water supply should be highlighted in the system of measures aimed at improving the living conditions and health status of children in the Aral Sea region. The quality of drinking water determines the increase in the direct and indirect influence of the water factor on the health of children.

In the Aral Sea region, children develop violations of the macro-and microelement status, the immune system, which under normal conditions are mobile, have a pronounced margin of safety and the information content of which is especially high.

A decrease in the quality of drinking water in the region affects the hemogram of children by increasing the content of leukocytes, as well as the relative and absolute content of lymphocytes, and reducing the relative and absolute content of monocytes. These changes, depending on the place of residence, are explained by the reaction of the immune system to environmental pollution in the region.

References:

1. Agadzhanyan N. A., Tsirkin T. Z., Chesnokova V. I., S. A. Human physiology. Medical book, 2009.– 528 p.
2. Atakhanova D. O., Madreymov A. M. Model of sanitary-epidemiological and environmental monitoring in the Republic of Karakalpakstan // Methodical recommendations. Nukus, 2017.– 10 p.
3. Akhmetova N. Sh., Tebenova K. S., Tuganbekova K. M., Rakhmetova A. M. Features of the immunogram in people living in ecologically unfavorable areas. The successes of modern natural science.– 2. 2013.– P. 9–11.
4. Bulatov V. P., Ivanov A. V., Rylova N. V. Influence of long-term use of drinking water of unfavorable mineral composition // Pediatrics.– No. 1. 2004.– C. 4–7.

5. Zaitseva N. V., Dianova D. G., Dolgikh O. V. Peculiarities of lymphocyte reactivity under conditions of exposure to heavy metals. "Вестник НГУ". Series: Biology, Clinical Medicine.– 10 (2). 2012.– P. 129–132.
6. Kamilova R. T. Age characteristics of somatometric development of schoolchildren living in Urgench // Med. zhurn. Uzbekistan.– No. 1–2. 2000.– P. 92–94.
7. Isaeva I. V., Shustova S. V., Maksinev D. V., Medvedeva G. V. To the question of gender and age characteristics of blood. Modern high technologies.– 4. 2005.– 45 p.
8. Mambetkarimov G. A., Zhiemuratova G. K. Methodological approaches to studying the influence of environmental factors in the Aral Sea region on the health of the population Materials of the international scientific-practical conference "Immunology-interdisciplinary problems".– Tashkent, 2014.– 9 p.
9. Mukhamedov T. M., Khalmetova R. T. Physical development of children in the ecologically unfavorable zone of the Aral Sea region according to the results of a retrospective study // Pediatrics.– No. 1. 2004.– P. 25–28.
10. Development of ecological methods for improving the health of the population in the region of Lake Aral. Research report. Center for Health Protection and Ecodesign LLP,– Astana, 2005.– 58 p.
11. Yan M., Wang Y., Tian Y., Lai Z., Yan L. Inhibition of allogeneic T-cell response by Kupffer cells expressing indoleamine 2,3-dioxygenase. World J. Gastroenterol.– 5 (16). 2010.– P. 636–640.
12. Secchiero P., Gonelli A., Mirandola P., Melloni E., Zamai L., Celeghine C., Melane D., Zauli G. Tumor necrosis factor-related apoptosis-inducing ligand induces monocytic maturation of leukemic and normal myeloid precursors through a caspase-dependent pathway. Blood.– 100. 2002.– P. 2421–2429.

https://doi.org/10.29013/ESR-22-5.6-16-20

Jiemuratova G.K.,
Institute of Immunology and Human Genomics,
Academy of Sciences of the Republic of Uzbekistan
Danilova E.A.,
Institute of Nuclear Physics, Academy of Sciences
of the Republic of Uzbekistan
Akhmedjanova Z.I.,
Institute of Immunology and Human Genomics,
Academy of Sciences of the Republic of Uzbekistan

FEATURES OF CHANGES IN SOME MICROELEMENTS IN CHILDREN OF THE ARAL SEA REGION

Abstract

Introduction. Deviations in the intake of macro and microelements by the human body, which adversely influence their ratios affecting their activity in the body, reduce or increase its resistance, and therefore the adaptability. The long-term chemical load has a significant impact on the content of the essential microelements in the body of people living in the Aral Sea region.

The purpose of the study. Determination of the content of macro and microelements in children's' hair living in the Aral Sea region is conducted.

Materials and research methods. To determine the content of macro and microelements, hairs samples of people living in Nukus city were examined. All children were divided into 4 age groups: group I consisted of children from new – born to 4 years of age, group II comprised children from 4 to 8 years old, group III consisted of children from 8 to 15 years old and group IV comprised children from 15 to 19 years old.

Determination of the content of essential microelements (chromium, manganese, iron, cobalt, copper, zinc, selenium, iodine, etc.) in the hair samples was carried out in the laboratory of activation analysis of the Institute of Nuclear Physics of the Academy of Sciences of the Republic of Uzbekistan by instrumental neutron activation analysis (INAA).

The results of the survey. While studying the elemental composition of children's hair from the abovementioned groups I, II, III and VI an imbalance in macro and microelements of varying degrees of severity was revealed. All examined children exhibited a statistically significant decrease in the content of Cu, Co, Zn, I and Cr in groups II, III, and VI. This indicates the increased probability of developing anemia and disorders in the gastrointestinal tract, endocrine and immune systems.

Comparison of the microelement analysis results of the hair samples of children and their parents (Tables 1 and 2 respectively) revealed that parents also exhibited a deficiency of Cu, Co, Cr, I, and Br. At the same time, an increased content of toxic element -uranium was revealed in children and parents, which indicates the occurrence of environmental pollution in the Aral Sea region.

Conclusion. The study confirms the potential promise of screening studies of macro and microelements in biosubstrates in various population groups in order to correct both the elemental status and improve the indicators of population health and quality of life in general.

Testing of various biological environments for the most common chemical environmental pollutants allows us to develop ways of preventing and correcting detected violations.

Keywords: hair, macro and microelements, neutron activation method, ecological factors, the Aral Sea region.

One of the most important and prerequisites for the normal functioning of an organism is the stability of its chemical composition.

Learning the effect of a deficiency or excess of microelements on the adaptation of the human body to environmental conditions and the occurrence of endemia is the subject and tasks of a new branch of science – biogeochemical ecology. Deviations in the intake of macro and microelements into the human body, violation of their ratios affect the activity of the body, reducing or increasing its resistance, and therefore the adaptability [1].

Anthropogenic impacts, including excessive intake of heavy metals, as well as endogenous and exogenous deficiency of vital chemical elements, which is observed in provinces of high environmental and biogeochemical risk, contribute to reduction of health at the individual and population levels, and in some regions, to an increase in depopulation [2; 3]. The main environmental factors affecting the health status of the Aral Sea region's population: desertification of the land, deficiency of pure drinking water, massive salinization of the land, chemical pollution of natural environments (water, air, soil, plants), increased air dryness and extreme temperatures. From this point of view, the systematic monitoring of the composition of the soil, plants, water, air, and other natural objects, raising awareness about the real environmental situation in the region, is relevant and important. A long-term chemical load has a significant effect on the content of essential microelements in the body of the population living in the Aral Sea region, particularly in Karakalpakstan [4; 5]. The most susceptible to diseases associated with the violation of macro and microelement status are children. This is due to their increased demand for essential microelements and their high sensitiveness to the toxic effects of heavy metals. In this regard, the study of macro and micronutrients' content, in children with physiological and pathological conditions and the possible impact of their imbalance on the condition of the child, is noteworthy [6].

Available data show that the content of microelements in the hair shows the microelement status of the organism as a whole and can serve as an integral indicator of the environment's condition [7].

Hair is the most appropriate material for medical and environmental studies. As a biological object of study, hair has an advantage over other biosubstrates. Their collection is simple, painless, so the hair is indispensable when conducting mass researches.

Currently, there are various modern methods for the determination of macro and microelements in human biosubstrates. Most of these methods require a sample decomposition procedure for the quantitative isolation of elements, which is often associated with possible sample contamination and with rather complicated sample preparation [1; 7].

The neutron activation method allows with high sensitivity and performance to determine more than 25 elements in one sample set, wherein sample preparation is quite simple and does not require sample decomposition. The main stages of instrumental neutron activation analysis are the selection of the optimal time regime (irradiation time, "cooling" time, measurement time) and spectrometry of the irradiated sample. The time regime should be selected so as to provide with the most useful signal and reduce the effect of radiation from interfering radionuclides and, at the same time, provide a sufficiently high analysis performance [1; 4].

The purpose of the survey.

Determination of the content of macro and microelements in children's' hair who are living in the Aral Sea region.

Material and research methods

To determine the content of macro and microelements, hairs of people who are living in the city of Nukus were examined. While working with patients, the ethical principles of the Helsinki Declaration of the World Medical Association (World Medical Association Declarationof Helsinki 1964, 2000) were followed.

Hair was cut from the occipital part of the head directly from the scalp with 3 cm long strands. It is known that hair grows at a speed of 1–1.5 cm per month, therefore, 3 cm long strand reflects the elemental status of the organism over the past 2–2.5 months. Cut hair was thoroughly washed in acetone, dried, weighed and packaged in labeled plastic bags. The prepared samples were subjected to neutron activation analysis.

All children were divided into 4 age groups: group I consisted of children from birth to 4 years, group II children from 4 to 8 years old, group III from 8 to 15 years old and group IV from 15 to 19 years old.

Analysis of the hair samples for the content of essential microelements (chromium, manganese, iron, cobalt, copper, zinc, selenium, iodine, etc.) was carried out in activation analysis laboratory at the Institute of Nuclear Physics, the Academy of Sciences of the Republic of Uzbekistan, by instrumental neutron activation analysis (INAA). The methods of preparing and conducting INAA have been described in detail in previous studies [3; 4]. The obtained data on the content of microelements in the hair of patients were compared with reference indices of practically healthy children aged 1 year to 18 years [10]. Statistical processing of the research results was carried out by the Student's t-criterion method of statistical analysis, using Excel 2010 and STATISTICA 6 software.

Results and discussion

The data on the content of microelements in the hair of children living in the Aral Sea region in accordance with the different age groups are listed in (table 1).

Table 1.– The content of elements in the hair of children living in the Aral Sea region in accordance with the different age groups (mkg/g)

Element	Examined children				Normal range	
	Group I 1–3years n=16	Group II 4–8 years n=14	Group III 9–14years. n=16	Group VI 15–19years. n=6	Minimum	Maximum
Cr	0.41±0.11	0.28±0.026	0.26±0.016	0.27±0.073	0.35	1.0
Mn	1.2±0.34	0.61±0.056	0.53±0.039	0.40±0.074	0.35	1.0
Fe	29±5.6	20±1.9	21±1.5	16±3.5	15	30
Co	0.020±0.0027	0.013±0.0034	0.022±0.0044	0.017±0.0034	0.02	0.11
Cu	6.9±0.97	6.6±0.89	7.5±1.0	7.2±1.0	10	15
Zn	83±14	120±73	120±8.1	170±18	150	250
Se	0.44±0.038	0.41±0.038	0.36±0.036	0.46±0.029	0.35	1.0
Br	4.7±0.96	2.6±0.40	1.3±0.23	1.0±0.16	1.0	3.0
I	0.61±0.30	0.61±0.16	0.17±0.055	0.22±0.12	0.8	1.5

When analysing the elemental composition of the children's hair samples from groups I, II, III, and VI, an imbalance in macro and microelements of varying degrees of severity was revealed, and each individual group possessedits own characteristic distinguishing features in each individual group.

In the first group (from new – borns to 4 years of age), the contents of manganese and bromine were higher than that those reported in the references. The increased contents of Br and Mn in Group I are connected with a high content of these elements in mothers during pregnancy, who had experienced problems of the cardiovascular and nervous systems [9].

According to the content of iron in the hair samples of children from groups I, II, III and VI, there were no significant differences ($p > 0.05$). The average concentration of iron in the hair samples of children from all age groups corresponded to the physiological norm, however, significant differences were observed between groups ($p < 0.05$).

In all examined children there was a statistically significant decrease in the content of Cu, Co, Zn, I, and Cr in groups II, III, and VI. First of all, this indicates the probability of developing anemia and disorders of the gastrointestinal tract, endocrine and immune systems.

Comparison of the microelement analysis results of the hair samples of children and their parents (Table 2) revealed that parents also exhibited a deficiency in Cu, Co, Cr, I, and Br and 35.3% of parents had an increased Mn.

Environmental pollution by toxic elements primarily affects children, since their intensive accumulation occurs even in the placenta of a pregnant woman. This leads to the occurrence of congenital malformations, a delay in mental and physical development, a decrease in immunity and the development of diseases, often with a chronization of the pathological process [10].

Table 2. – The content of macro and microelements in the hair samples of parents living in the Aral Sea region (mkg/g)

Element	Surveyed parents	Normal range (A. V. Skalny. 2004)	
		Minimum	Maximum
Cr	0.34±0.028	0.35	1.0
Mn	1.2±0.32	0.35	1.0
Fe	23±3.7	20	30
Co	0.029±0.0052	0.05	0.15
Cu	6.8 ±0.73	10	15
Zn	170±19	150	250
Se	0.39±0.033	0.35	1.0
Br	0.92±0.15	1.0	3.0
I	0.22±0.095	0.8	1.5

Conclusion

Accumulated data support the prospect of screening studies of macro and microelements in biosubstrates in different population groups with the aim of correcting both elemental status and improving indicators of population health and quality of life in general.

Testing of various biological environments for the most common chemical environmental pollutants allows us to develop ways of preventing and correcting detected violations.

Deviations in the content of chemical elements caused by environmental, occupational, climatic and geographical factors or diseases lead to a wide range of health disorders. In this regard, the identification and assessment of deviations in the exchange of macro and microelements, as well as their correction, are a promising area of modern medicine that allows us to approach the solution of many theoretical and especially practical issues that significantly affect the health indicators of the population of the regions, which differ sharply in terms of economic, social development, climatic and geographical and biogeochemical conditions.

References:

1. Agadjanyan N. A., Suslikov V. L., Ermakova N. V., Kaplanova A. Sh. (2015) Microelement deficiency and children's health problems. Pediatrics,– Vol. 94.– No 6.– 224 p.
2. Ismailova Sh. T., Makhmudova D. I., Salikhova K. Sh. Comparative analysis of the content of toxic metals in hair and other human biosubstrates Microelements in medicine – 10(1–2). 2009.– P. 88–90.
3. Lux A., Martinka M., Vaculik M., White P. J. Root responses to cadmium in the rhizosphere: a review. J. Exp. Bot.– Vol. 62.– No. 1. 2011.– P. 21–37.
4. Jumamuratov A. The neutron-activation method in the study of the geochemical and agrochemical state of irrigated soils of the Aral Sea region and ways to improve it. abstract dissertation Doctor of agricultural sciences / A. Jumamuratov; – Tashkent, 2011.– 42 p.
5. Jumamuratov M. A. Clarks of the concentration of certain chemical elements in the bottom sediments of the Karakalpak region // Universum: Chemistry and Biology: Electron. scientific journal – 3 (57). 2019.
6. Eremeishvili A. V., Firago A. L. = Ecological – biological monitoring of the microelement status, development and health status of children aged 1 to 3 years in an industrial city (on the example of the city of Yaroslavl). Modern High-Tech Technologies Journal.– 7. 2010.– P. 186–190.
7. Chojnacka K., Michalak I., Zielinska A. et al. Interrelationship between elements in human hair: the effect of gender // Ecotoxicol. Environ Saf.– Vol. 73.– No. 8. 2010.– P. 2022–2028.
8. Sloiewski M., Czerny B., Safranow K. et al. Microelements in stones, urine, and hair of stone formers: a new key to the puzzle of lithogenesis? // Biol. Trace Elem. Res.– Vol. 137.– No. 3. 2010.– P. 301–316.
9. Mircoelement of iron in the Aral Sea region and weekly ferro-complementation in the most vulnerable groups of the population: abstract of thesis. Dr. med. Sciences: 14.00.07 / R. A. Shakieva; Kazakh Academy of Nutrition.– A., 2005.– 50 p.– state number Registration OD53.28.01.
10. Namazbaeva Z. I. Sakiev K. Z. Ibraeva L. K. Ibraibekova A. M. Iskendirova A. Zh. The content of microelements in children of the Aral Sea region. Journal of Occupational Hygiene and Medical Ecology.– 3 (48). 2015.– P. 58–62.
11. Namazbaeva Z. I., Sabirov Zh.B., Darkesheva A. M., Berjanova R. S., Pochevalov A. M. Microelement status of the Aral Sea population. Occupational medicine and human ecology,– 3. 2017.– P. 38–42.

Section 3. Pedagogy

https://doi.org/10.29013/ESR-22-5.6-21-24

Terzieva Galena Todorova,
Assistant Professor, PhD in Pedagogy,
the Faculty of Education
Trakia University, Stara Zagora, Bulgaria

ADAPTATION OF MOBILE GAMES FOR CHILDREN WITH HEARING IMPAIRMENTS

Abstract. The aim of the article is to study the degree of mastery by the respondents of the method of Lieberman and Houston-Wilson for the adaptation of mobile games for children with hearing impairments. 41 third-year students majoring in Pre-school and Primary School Pedagogy are participating. The training is carried out during the summer semester of the academic year 2020/2021. It is conducted online and includes the following methods – lectures, discussions, case studies.

The summarized results show that 73.1% of the respondents have a high level of adaptations to the method. 22% of the students have some gaps in two or more areas, and 4.9% show a low level of skills.

Keywords: inclusive education, adapted physical education, pedagogical students.

The main goal of the Bulgarian Sign Language Act, in force since 2021, is to form sustainable attitudes and motivation for lifelong learning and to ensure equal opportunities for deaf people to fully integrate and participate in public life. An important principle enshrined in it is equal access to quality education [2]. The main prerequisite for the optimal organization of the learning process in the mainstream school is overcoming the communication difficulties caused by hearing impairment [3, 86]. The possibilities for overcoming these obstacles now seem to be greater, as greater participation of an interpreter in the education and training in Bulgarian sign language for hearing children is envisaged. Inclusion must take place in all areas, including physical education. Mobile games are the most used means of motor learning in preschool and primary school age. Well-thought-out and organized play creates speech stimuli and favorable conditions for verbal communication between children, enriches vocabulary, expands motor skills, develops mental qualities, stimulates initiative and independence of hearing-impaired children, creates mood and partnership in the group [4, 177; 7, 60].

There are various methods for adapting mobile games for children with hearing impairments. The method of Lieberman and Houston-Wilson [5, 83–86] is introduced in the education of students majoring in Pre-school and Primary School Pedagogy. According to him, the changes are taking place in four main directions:

- Adaptation of the environment – includes all changes that reduce distraction, reduce noise, adjust lighting, increase visual signals and create optimal accessibility to the playground for children with disabilities.

- Adaptation of the equipment – involves modification of the devices used in the games, which allows the successful inclusion of children with disabilities, as they are tailored to their needs and capabilities. They can also be used by children without disabilities, without hindering their motor development.
- Adapting the rules of the game – there are many options for which one game can be played. The change is aimed at simplifying or creating alternative rules so that all children, including those with disabilities, are successfully included.
- Adaptation of instructions is associated with changes in the teaching methods. The correct selection, combination and modification of the methods for motor training is sought – verbal, visual, auxiliary-motor and tactile.

Following the method of Lieberman and Houston-Wilson and the guidelines given by various authors to modify physical activity [1, 220–223; 6, 109–116; 8, 83; 9, 261–264], the following possibilities for adapting mobile games for children with hearing impairments are outlined:

For the environment:

- Enable a child with residual hearing to use it while minimizing background noise.
- As it compensates for the lack of hearing and sight, it is necessary to take into account where the activities take place – outdoors the child stands so that the sun does not interfere with seeing what is happening, indoors – the playground is well lit.
- All important areas in the playground, as well as the facilities that are part of the game, should be of such a color as to ensure maximum visibility and orientation in the space of the child with hearing impairment.

For equipment:

- Also, for better visibility, all devices used in the game should be in well-distinguished colors.
- When there is residual hearing, sound-emitting devices can be used for better orientation.
- If the game is musical, the use of additional devices helps to better feel the vibrations.

About the rules of the game:

- All sound signals are replaced with visual ones – at the beginning and end of the activity, when giving instructions, commands or hints during the game.
- If there is residual hearing, the signals may be audible, but the teacher should be as close as possible to the child to make sure he or she can hear.
- If the child has a hearing aid or cochlear implant, it is possible to change the rules of the game so that there is no risk of breaking and injuring the child.
- Other children are used as helpers.
- When the game involves the division of teams, they should be in very well distinguishable and distinctive equipment.

For instructions:

- The child's preferred means of communication should be used – sign language, lip reading.
- If you do not learn the basic gestures of communication, an interpreter can be used.
- If the child reads on the lips, speak clearly and concretely and look in the face.
- The main method used for deaf children is demonstration.
- All actions that are shown are to be performed in the child's field of vision.
- All kinds of visual aids are used to ensure maximum understanding of the rules of the game – various visual aids that have images and text.
- If video is used, it must be captioned.
- Verbal methods may also be used in children with residual hearing or using a hearing aid or a cochlear implant.
- Feedback is always sought in the direction of understanding the rules of the game and the organization of the performance.

The aim of the article is to study the degree of mastery by the respondents of the method of Lieberman and Houston-Wilson for the adaptation of mobile games for children with hearing impairments. 41 third-year students majoring in Pre-school and Primary School Pedagogy are participating. The training is carried out during the summer semester of the academic year 2020/2021. It is conducted online and includes the following methods – lectures, discussions, case studies. Through the analysis of the decisions of the cases it is established to what extent the skills to adapt the environment, the equipment, the rules and the instructions are formed. The assessment for each area is based on a three-level scale: he or she can, can to some extent, can't. The summary shows the extent to which – high, medium, low – students master the adaptation of mobile games for hearing-impaired children by the method of Lieberman and Houston-Wilson.

80.5% of the respondents do not have any difficulties in adapting the playground according to the peculiarities of children with hearing impairments. 14.6% do not take into account the recommendations related to the use of residual hearing and ensuring maximum visibility, and 4.9% of students do not cope with this task at all.

The same is true of changing the appliances used. 80.5% of the participants took into account all the features of children with varying degrees of hearing impairment, 14.6% have small gaps related to the activation of all working senses in the selection of equipment, and 4.9% – significant ones.

68.3% of the respondents are able to make any changes in the rules of the games for the successful and full inclusion of children with hearing impairments, and 7.3% – do not know how. 24.4% of the respondents partially cope with this challenge, as their problems are related to the selection of appropriate visual aids in order to create preconditions for equality, compliance with the rules, contra-indications for physical activity of hearing-impaired children and lack of on the sense of when it is most appropriate to include an assistant.

56.1% of the students choose the appropriate means of communication according to the preferences of the child with hearing impairment and correctly combine the possible teaching methods. Unfortunately, over 1/3 of the participants (36.6%) experience some difficulties in performing these activities, and 7.3% – significant ones.

The summarized results show that 73.1% of the respondents have a high level of adaptations to the method. 22% of the students have some gaps in two or more areas, and 4.9% show a low level of skills. These are the participants who do not fully consider the possibilities or try to make adaptations without reading and thinking about all the recommendations and guidelines that are given when working with children with hearing impairments.

The method of Lieberman and Houston-Wilson is suitable for adapting mobile games for children with hearing impairments, as it creates the preconditions for overcoming communication difficulties by selecting appropriate ways of communication and instruction. It also allows you how to modify the rules, equipment and playing area according to the needs and abilities of children. It is no coincidence that a high percentage of the students were excellent in solving cases, although the training was conducted only online. Theoretically, they form a base of skills for the inclusion of hearing-impaired children in mobile games, which will be upgraded in their future real work related to the processes of inclusion of this group of children.

References:

1. Block M. A Teacher's Guide to Including Students with Disabilities in General Physical Education. Baltimore, – Maryland, 2016.
2. Bulgarian Sign Language Act, in force since 06.02.2021 – URL: https://www.lex.bg/bg/laws/ldoc/2137209455
3. Georgiva D., Valchev G. Specific features of interpersonal communication in deaf children. CBU International Conference Proceedings "Innovations in science and education", Prague, Czech Republic,– Vol. 8. 2020.– P. 81–87.
4. Ivanova V., Siderova D. Projections of the game with motional performances in the process of literary communication at pedagogical interaction with 6–7 years old children. Activities in Physical Education and Sport.– 3 (2). 2013.– P. 174–177.
5. Lieberman L., Houston-Wilson C. Strategies for inclusion: physical education for everyone.– Human Kinetics, 2018.
6. Rouse P. Inclusion in physical education.– Human Kinetics, 2009.
7. Shapkova L. V. Corrective outdoor games and exercises for children with developmental disabilities.– Moscow.
8. Van Coppenolle H. Count me in – A guide to Inclusive Physical Activity, Sport and Leisure for Children with a Disability.– Leuven, 2006.
9. Winnick J., Porretta D. Adapted Physical Education and Sport. Human – Kinetics, 2017.

Section 4. Physics

https://doi.org/10.29013/ESR-22-5.6-25-28

Daliev Shakhrukh Kh.,
leading researcher of Institute of Semiconductor Physics and Microelectronics of National University of Uzbekistan
Tashkent, Republic of Uzbekistan
Ergashev Javokhir A.,
PhD student of Research Institute of semiconductor physics and microelectronics
Tashkent, Republic of Uzbekistan

DEEP LEVEL TRANSIENT SPECTROSCOPY OF DEFECTS IN SILICON MULTILAYER STRUCTURES DOPED WITH HAFNIUM ATOMS

Abstract. By means of methods transient capacitance spectroscopy of deep levels has been used to study defect formation in silicon multilayer structures doped with hafnium atoms. It has been established that the presence of electrically active hafnium atoms in the silicon substrate of the MIS structures leads to an increase in the density of the surface states N_{ss} and the appearance of distinct peaks caused by hafnium atoms with deep levels of E_c-0.23 eV and E_c-0.28 eV on n-Si<Hf> and Ev+0.35 eV on p-Si<Hf>. The presence of an electroneutral hafnium impurity in the silicon substrate of the MIS structures does not lead to a change in the density of the surface states of the MIS structures and the DLTS spectra.

Keywords: spectroscopy, silicon, defect, deep level, doping of the impurity, Hafnium, MIS structures.

Introduction

It is known that the doping of silicon with high melting elements significantly affects the performance characteristics of semiconductor devices [1–4]. In addition, there are contradictory data in the literature on the electrical activity of these impurities and their interaction with other defects. In most works there is no information about the electrical activity of these atoms. It is known that high melting elements introduced into silicon from the melt during cultivation, having high chemical activity and a tendency to complexation, are present in silicon in an electrically inactive state.

The processes of doping of semiconductor materials and multilayer structures with acceptor and donor impurities that create shallow levels have been studied quite fully [5], as for doping with impurities of high melting elements, due to the complex nature of the interaction between impurity particles and defects in the semiconductor structure, the influence of heterogeneity of the structure of metal-insulator -semiconductor structures (MIS structures) on redistribution impurities, there is not enough clarity here [6]. It is the presence of such impurities that is associated with the stability of the operating parameters of microchips based on MIS structures.

Experimental part

This work is devoted to the study of the influence of one of the high melting elements – hafnium on the electrophysical properties of silicon multilayer structures of the metal- insulator -semiconductor type (MIS structures) with thermally grown oxide. Silicon doping with hafnium was carried out both by diffusion method and in the process of growing from the melt.

Diffusion doping of silicon with hafnium was carried out in the temperature range 1000 ÷1200 °C for 10 hours from a metal hafnium layer deposited on the Si surface. Then, on plates of n-Si<Hf> with a resistivity of ρ = 10÷40 Ohms cm, a layer of SiO_2 with a thickness of about 800÷850Å at 900 °C was thermally grown in an atmosphere of moist oxygen. By thermal spraying of aluminum on a layer of silicon dioxide, metal electrodes were created, their area was 0.03 cm^2, thickness – 7000 Å.

To study various defects created by Hf atoms and their influence on the properties of the volume and the Si-SiO_2 interface of silicon MIS structures, we conducted comprehensive studies using methods of deep level transient spectroscopy spectroscopy in the constant capacitance mode (CC-DLTS) and high-frequency volt-farad characteristics (C–V characteristics). The concentration of possible deep levels in the silicon volume was measured by the C-DLTS method on Schottky barriers made on silicon after the SiO_2 layer was etched [7–8].

Results and its discussion

From measurements of the volt-farad characteristics of MIS structures based on silicon diffusionally doped with hafnium, it was found that they are shifted towards negative displacements compared to the control MIS structures. This indicates that the diffusive introduction of hafnium into silicon leads to an increase in the density of the surface states of the MIS structures and the formation of a positive charge at the Si-SiO_2 interface.

Measurements of CC-DLTS spectra in Si-based structures doped with hafnium in the process of growing from the melt and control MIS structures (without hafnium impurity) showed that their spectra practically coincide and there is no noticeable concentration of any deep levels, although according to neutron activation analysis, the content of hafnium atoms is quite high, of the order of $2\times10^{16}\div5\times10^{18}$ cm^{-3}. This indicates that after doping silicon with hafnium during the growing process, no deep levels are formed in the forbidden zone of the silicon substrate. Consequently, the hafnium atoms introduced during the growing process are in the silicon volume in electron-neutral states.

Studies have shown that they can be activated using high-temperature treatments. At the same time, the energy spectrum of deep levels is similar to samples doped with hafnium by diffusion method (Fig. 1, curve 2). Note that the concentrations of deep levels bound to Hf atoms in $Si\langle Hf\rangle_{diffusion}$ samples (Fig.1, curves 3 and 4) are an order of magnitude higher than in $Si\langle Hf\rangle_{growing}$ samples.

Analysis and measurement of CC-DLTS spectra of MIS structures based on silicon diffusionally doped with hafnium (Fig. 1, curves 3 and 4) and control MIS structures (Fig. 1, Curve 1) showed that 2 peaks with maxima at temperatures T_{max} = = 110 K and T_{max} = 146 K, and no such peaks were found in the control samples. Numerical calculations of the parameters of defects caused by these peaks showed that the peak with a maximum at T = 110 K corresponds to the level with an ionization energy of E_c – 0.23 eV, and the peak at T = 146 K corresponds to the level with an ionization energy of E_c – 0.28 eV.

Measurements of the density distribution of N_{ss} surface states over the band gap width of the semiconductor units of silicon MD structures with and without hafnium impurity have shown that the distribution spectrum of the dependence of N_{ss} on E_g has a typical U-shaped character. Analysis of these dependencies showed that the presence of hafnium in the substrate does not lead to noticeable changes in the distribution of N_{ss} over E_g and the formation of any pronounced peaks.

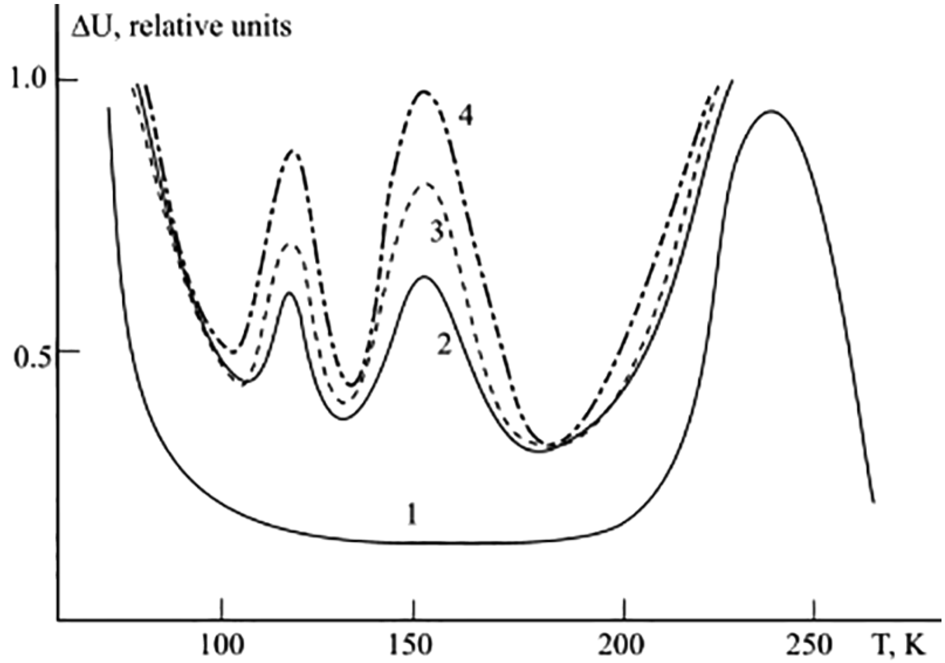

Figure 1. CC-DLTS spectra in MIS structures with Hf introduced at growing (curve 1), at growing+ heat treatment (curve 2) and introduced by diffusion (curves 3, 4)

It is established that the presence of electrically active hafnium atoms in the substrate of multilayer structures of the Al-SiO_2-n-Si<Hf> type leads to noticeable changes in the CC-DLTS spectra and two pronounced peaks in the energy range with values of E_c – 0.23 eV and E_c – 0.28 eV are observed on the spectra in doped structures. To identify these defects with certain impurities, SiO_2 layer was removed in the studied MIS structures and Schottky barriers were made on them. Gold was sprayed onto the n-Si<Hf> substrate as a Schottky barrier, and antimony was sprayed in high vacuum as an ohmic contact.

Typical DLTS spectra of the n-Si<Hf> and p-Si<Hf> samples measured at the obtained barriers were similar to the spectra in Fig.1. Processing of the DLTS spectra and their analysis show that in the n-Si<Hf> samples, two deep levels with ionization energies E_c – 0.23 eV and E_c – 0.28 eV. In the samples of p-Si<Hf>, one deep level with an ionization energy of E_v+0.35 eV was detected. Analysis of the DLTS spectra showed that the levels with the ionization energy E_c – 0.28 eV and E_v+0.35 eV are associated with hafnium atoms in Si. These results confirm the data obtained from measurements of CC-DLTS spectra.

Conclusion

Thus, the analysis of the obtained results shows that the parameters of deep levels in MIS structure do not differ from the parameters of the corresponding levels observed in Si diffusionally doped with hafnium.

It has been established that the presence of electrically active hafnium atoms in the silicon substrate of the MIS structures leads to an increase in N_{ss} and the appearance of distinct peaks associated with hafnium atoms, and the presence of an electroneutral hafnium impurity in the silicon substrate of the MIS structures does not lead to a change in the density of the surface states of the MIS structures and the DLTS spectra.

References:

1. Lemke H. Titanium in Silicon. Symposium MRS, F: Materials Issues in Silicon Integrated Circuit Processing,– Vol. 71. 1986.– P. 197–199.
2. Roth T. F., Rudiger M., Stefan W. Glunz. Titanium-related defect levels in silicon analyzed by temperature-dependent photoluminescence lifetime spectroscopy. 33rd IEEE Photovoltaic Specialists Conference,– 11–16. May, 2008.– P. 29–32.
3. Codegoni D., Polignano M. L., Caputo D., Riva A. et.al. Molybdenum Contamination in Silicon: Detection and Impact on Device Performances. Solid State Phenomena.– Vols. 145–146. 2009.– P. 123–126.
4. De Luca A., Texier M., Burle N., Oison V., Pichaud B., Portavoce A. Tungsten diffusion in silicon. Journal of Applied Physics,– Vol. 115.– Issue 1. 2014.– P. 208–213.
5. Ravey K. Defects and impurities in semiconductor silicon // – Moscow: Mir, 1984.– 475 p. Translated from English. ed. Gorina S. N.
6. The Rumak N. In. The system silicon-silicon dioxide in MOS structures (Minsk; Science and technique). 1986.
7. Lebedev A. A., Ecke W. 1985 Semiconductors – 19. 1087. (in Russian).
8. Daliev Kh. S. Utamuradova Sh. B., Daliev Sh. Kh. Technical Physics Letters,– 32. 2006.– 469 p. Pleiades Publishing, Inc.

https://doi.org/10.29013/ESR-22-5.6-29-32

Mahliyoxon Adxamovna Mamatova,
doctoral student of Fergana State University
Rasulov Rustam Yavkachovich,
professor of Fergana State University,
Mirzaakbarov Dilshodbek,
lecturer at Ferghana State University.
Kasimov Forrukh,
teacher at Andijan State University.

RELATION BETWEEN THE CONCENTRATION OF NONEQUILIBRIUM ELECTRONS AND HOLES IN LONG SEMICONDUCTOR DIODES

Abstract. Analytical expressions are obtained for the dependence of the concentration of nonequilibrium current carriers on the parameters of deep impurities in compensated semiconductors, where the capture of carriers to deep impurity levels is taken into account. It is pointed out that the relationship between the concentration of nonequilibrium carriers is greatly complicated due to the variety of recombination processes and the generation of current carriers through multiply charged impurities. In this connection, below we analyze the dependences of nonequilibrium electrons and holes on the parameters of deep impurity centers.

Keywords: nonequilibrium current carriers, deep impurity centers, recombination and generation through multiply charged impurities.

At present, progress in the field of power semiconductor electronics is largely determined by the creation of devices with an optimal combination of electrical characteristics. The interrelation of various characteristics of devices, on the one hand, makes it difficult to carry out optimization calculations, and on the other hand, it requires an increase in the accuracy of theoretical calculations. From this point of view, the possibilities of some analytical calculations containing a number of significant simplifications (for example, the division of a semiconductor structure into regions of a strong field and quasi-neutral regions, the use of various approximations in solving the continuity equation, etc.) turn out to be clearly insufficient for an adequate description of the processes of charge carrier transport in multilayer semiconductor structures in a wide range of changes in external conditions (temperature, deformation, radiation) and parameters that determine the operating mode of the device (forward current density, voltage, etc.). Under these conditions, the only possible way out is the transition to exact approximations based on the solution of the fundamental system of equations of a semiconductor device by difference methods. Such approximations make it possible to take into account the complex profiles of the distribution of various electrophysical parameters over the thickness of the semiconductor structure. A large volume of literature devoted to the numerical simulation of semiconductor structures published in recent years indicates the promise of this direction [1; 2].

The current-voltage characteristic (CVC) S – of the type in three-layer structures in a diode connection, the base of which is made of a compensated semiconductor, is described not only by a mechanism due to a nonlinear increase in the conductivity of the semiconductor thickness (base) depending on the current, but also by mechanisms due to an increase [3; 4]: the rate of thermal generation of carriers due to the heating of the thickness of the semiconductor by the flowing current; injection coefficient $p-n$-transition with increasing current; carrier mobility in a strong electric field upon scattering by ionized impurities [5]; lifetime with increasing carrier concentration (τ – mechanism) [6].

It is easy to verify that the proportion of the above mechanisms in the formation of negative resistance in diodes from semiconductors with deep impurity levels is determined by the dependence of nonequilibrium electrons and holes. This is due to the fact that in diodes, the base thickness of which is much larger than the diffusion length, the distribution of injected carriers depends on nature, in particular, on the degree of impurity charge. Therefore, the influence of the electric field on the distribution of nonequilibrium carriers in the base of the diode changes sharply with an increase in the injection level. But, in a purely intrinsic semiconductor, the field does not affect the distribution of current carriers at all.

In compensated semiconductors, due to the capture of carriers to deep impurity levels, the relationship between the concentration of nonequilibrium carriers is greatly complicated due to the variety of recombination processes and the generation of current carriers through multiply charged impurities. In this connection, we will analyze below the dependences of the concentration of nonequilibrium electrons and holes on the parameters of deep impurity centers.

Gold atoms in silicon can be in minus, zero, and plus charge states. The acceptor and donor levels are located above the valence band by 0.62 and 0.35 eV, respectively [7]. To determine the relationship between the concentrations of electrons and holes and the recombination rate, we assume that the transition processes occur according to the following scheme

$$Au + \rightleftarrows A^-; \mathrm{Au}^+ + e \rightleftarrows Au,\ Au + h \rightleftarrows Au^+;$$
$$Au^- + h \rightleftarrows Au, \qquad (1)$$

where e (h) are electrons (holes).

These processes of recharging gold atoms by carriers are characterized by some probabilities W_{0-}, W_{+0}, W_{0+}, W_{-0}, which are equal to the capture cross sections of the corresponding processes, multiply by the average thermal velocity of an electron or hole and by the total concentration of gold atoms. Thermal generation and carrier recombination through the band gap are not taken into account. Expressions (1) lead to the following kinetic equations for charged gold atoms

$$\frac{dNf_-}{dt} = f_0 W_{0-}(n+n_0) - f_- W_{-0}(p+p_0) - \mathrm{A} f_- N + B f_0 N,$$
$$\frac{dNf_+}{dt} = f_0 W_{0+}(p+p_0) - f_+ W_{+0}(n+n_0) - C f_+ N + D f_0 N. \qquad (2)$$

Here, N, $n(n_0)$ and p (p_0) are the concentrations of gold, non-equilibrium (equilibrium) electrons and holes, $f_{-1,}$ f_0 and f_+ are the fractions of minus-, zero- and plus-charged gold atoms.

Coefficients A, B, C, and D characterizing the rate of thermal generation of carriers from impurity centers are determined from the principle of detailed equilibrium between levels and bands through the parameters of an equilibrium semiconductor $A = \frac{f_0^0 W_{0-} n_0}{N f_-^0}$, $B = \frac{f_-^0 W_{-0 p_0}}{N f_0^0}$, $C = \frac{f_0^0 W_{0+p_0}}{N f_+^0}$, $D = \frac{f_+^0 W_{+0 n_0}}{N f_0^0}$, where the index "0" means the equilibrium value of the considered parameters. Then, using the obvious equality from the solution of system (2), one can easily obtain the following relations

Using the obvious equality

$$f_0 + f_- + f_+ = 1,$$

from the solution of system (2) for the stationary case, we obtain

$$f_0 = \frac{1}{a};\ f_- = \frac{1}{a}\frac{n+n_0+\theta\delta p_0}{\theta(\mathrm{p}+\mathrm{p}_0)+\delta^{-1} n_0};$$
$$f_+ = \frac{1}{a}\frac{p+p_0+\beta^{-1}\alpha n_0}{\alpha(n+n_0)+\beta p_0}, \qquad (3)$$

here

$$a = 1 + \frac{n+n_0+\theta\delta p_0}{\theta(p+p_0)+\delta^{-1} n_0} + \frac{p+p_0+\beta^{-1}\alpha n_0}{\alpha(n+n_0)+\beta p_0},$$

$$\alpha = \frac{W_{+0}}{W_{0+}};\ \theta = \frac{W_{-0}}{W_{0-}};\ \beta = \frac{f_0^0}{f_+^0};\ \delta = \frac{f_-^0}{f_0^0}.$$

The relationship between the electron and hole concentrations is determined by solving the following Poisson equation $\frac{dE}{dx} =$

$$= -\frac{4\pi e}{\varepsilon}\left\{ n - p - N\cdot f_-^0 + N\frac{n + n_0 + \theta\delta\cdot p_0}{\theta\cdot p + n + \theta(1+\delta)p_0 + (1+\delta^{-1})\cdot n_0} \right\}, (4)$$

where the concentration of shallow donors is obviously equal to

$$N_d = N\left(f_-^0 - f_+^0\right) + n_0 - p_0. \quad (5)$$

If we use the inequality $\frac{1}{n+n_0}\frac{\varepsilon}{4\pi\varepsilon}\frac{dE}{dx} \ll 1$, i.e. quasi-neutrality conditions, then from expressions (4) and (5) for silicon n – type we obtain

$$n = -\frac{\left[p(\theta-1) + A - N(f_-^0+1)\right]}{2}\left[1 + \sqrt{1 + \frac{4\left[p\left(\theta\cdot p + \theta\cdot N\cdot f_-^0 + A\right) + N\left(-B + A\cdot f_-^0\right)\right]}{\left[p(\theta-1) + A - N\cdot f_-^0 + N\right]^2}}\right]. \quad (6)$$

A similar expression can be obtained for the case with one acceptor level. This is a consequence of the fact that in n – type silicon, the charge state of gold is practically not realized either in equilibrium ($f_+^0 = 0$ due to the proximity of the donor level to the valence band), or in the stationary state (due to the large electron capture cross section for this state of gold $\alpha \gg 1$) [7].

To simplify further calculations of the distribution of current carriers along the length of the base, it must be assumed that the following condition is satisfied

$$\frac{1}{\theta+1}\left|\frac{N(\theta f_-^0 - f_0^0)}{N\cdot f_0^0 + \theta(1+\delta)p_0 + (1+\delta^{-1})n_0}\right| \langle 1. \quad (7)$$

In this case, the compensation of low-resistance silicon n – type occurs due to the filling of the acceptor level of gold with electrons from small donor impurities, and since the acceptor level of gold is located slightly above the middle of the band gap, it will be less than half filled in compensated silicon ($\delta < 1$). Then the dependence of the concentration of electrons and holes is described by the expression

$$n = p\frac{p + N_1}{p + N_2}, \quad (8)$$

where $N_1 = \frac{\theta\cdot N\cdot f_-^0 + \theta(1+\delta)p_0 + (1+\delta^{-1})n_0}{\theta+1}$,

$$N_2 = \frac{\theta\cdot N\cdot f_0^0 + \theta(1+\delta)p_0 + (1+\delta^{-1})n_0}{\theta+1}.$$

In conclusion, we note that the rate of hole recombination, i.e. the total number of holes captured per unit volume per unit time is described by the following expression

$$R_p = \left(W_{-0}f_- + W_{0+}f_0\right)p. \quad (9)$$

In conclusion, we note the following. Substituting (8) into (9) have a simple physical meaning. At low hole concentrations, the quantities f_- and f_0 in Eqs. (2) and (9) can be replaced by their equilibrium values. In particular, at $n = \theta\delta p$ (9) takes the form $R_p = \left(f_-^0 W_{-0} + f_0^0 W_{0+}\right)p$. At hole concentrations satisfying $p > \frac{N}{1+\theta}$ the following condition, the impurity states of gold are recharged, and now there should be more electrons than holes, just by the amount of the formed uncompensated charge, and the recombination rate will be determined by the corresponding stationary values of the fractions of minus and zero-charged atoms of deep impurities in the equilibrium state. Thus, the difference between the electron and hole concentrations increases from the equilibrium electron concentration to $N\left(\theta f_-^0 - f_0^0\right)$. This means that in this case the nonequilibrium concentration of nonequilibrium electrons can exceed the concentration of equilibrium ones by several orders of magnitude. In this case, the lifetime of holes will change from $\tau_1 = \frac{1}{f_-^0 W_{-0} + f_0^0 W_{0+}}$ to $\tau_2 = \frac{\theta+1}{W_{-0} + \theta W_{0+}}$.

References:

1. Gurin N. T., Korneev I. V., Maksin A. N., Novikov S. G. Position-sensitive combined device with *N*-shaped current-voltage characteristic // Proceedings of the IV Russian seminar on fiber lasers.– Ulyanovsk: UlGU2010.– 125 p. (in Russian).
2. Kashtankin I. A., Turin N. T. Temperature characteristics of bipolar *N*-devices with a controlled current-voltage characteristic // Nano- and microsystem technology.– No. 6. 2006.– P. 41–43. (in Russian).
3. Adirovich E. I., Karageorgy-Alkalaev P. M., Leiderman A. Yu. Double injection currents in semiconductors.– M.: Soviet Radio, 1978.– 320 p.
4. Stafeev V. I., Vikulin I. M. S-diodes semiconductor devices and their application / Ed. Ya. A. Fedotova.– M.: Sov. Radio.– No. 28. 1974.– P. 28–56. (in Russian).
5. Kazarinov R. F., Skobov V. G. On the theory of nonlinear galvanomagnetic phenomena in semiconductors.– ZhETF,– Vol. 42.– No. 4. 1962.– P. 1047–1053. (in Russian).
6. Stafeev V. I. The influence of the resistance of the thickness of a semi-conductor on the form of the current-voltage characteristic of the diode. ZhTF,– Vol. 28. – No. 8. 1958.– P. 1631–1641. (in Russian).
7. Milnes A. Impurities with deep levels in semiconductors. Monograph.– M.: Mir.–1977.– 568 p. (in Russian).

https://doi.org/10.29013/ESR-22-5.6-33-36

Rasulov Voxob Rustamovich,
Docent, of Fergana State University
Rasulov Rustam Yavkachovich,
Professor of Fergana State University
Mamatova Mahliyo Adhamovna,
PhD Research Scholar of Fergana State University
Khudoyberdiyeva Muhayyoxon Zoirjon-kizi,
PhD Researcher of Fergana State University
Mamadaliyeva Nargiza Zokirjon-kizi,
PhD, Teacher of Kokand State Pedagogical Institute

INFLUENCE OF A STRONG ELECTRIC FIELD ON THE CURRENT-VOLTAGE CHARACTERISTIC OF THREE-LAYER SEMICONDUCTOR STRUCTURES IN A DIODE CONNECTION

Abstract. The effect of an external electric field on the current-voltage characteristics of a three-layer semiconductor structure in a diode connection is calculated. It is assumed that the base of this structure is made of a compensated semiconductor, where there are three: zero, minus and charged impurities. It is taken into account that, in this case, the dependence of the electron and hole concentrations is nonlinear.

Expressions are obtained for the current-voltage characteristic of a long three-layer semiconductor for structures of the following types: *p+–n–n+, p+–n–p+, n+–n–n+* etc.

Keywords: external electric field, current-voltage characteristic, three-layer semiconductor structure, compensated semiconductor, impurities.

One of the main trends in the development of modern semiconductor electronics is the search and study of new modes of operation of bipolar multilayer semiconductor structures. This trend can be traced both in the analysis of the development of new semiconductor devices: high-power silicon energy converters [1–3], ultrafast switching transistors [4], and drift diodes [5], and in the analysis of the operation of traditional devices, including diodes.

The dynamics of transient processes in diode structures have been studied in many works. In the vast majority of these works, the description of the dynamics of processes was carried out in the framework of either a quasi-neutral diffusion approximation or a quasi-neutral drift approximation [6]. At the same time, when studying dynamic transient processes in the quasi-neutral approximation, the dependence of the mobility of charge carriers and the coefficient on the electric field strength in three-layer semiconductor structures, in which the base is made of a compensated semiconductor, was not taken into account.

At first glance, this approach seems to be quite justified, since, in stationary and dynamic modes, the magnitudes of the external electric field strength are, as a rule, small. However, as the current density increases, the characteristic values increase, and it can be expected that taking into account the dependence of the current carrier mobility may be necessary for the correct analysis of transient processes in ultrafast switching of specific cases, for example, on the types of semiconductor structures [7]. This assumption is confirmed in the description of the quasineutral approximation (, where the traditional equations for current carrier flows are used. The results obtained in the framework of this approach describe well the experimental data at not too high current densities. However, the very first attempts to study the problem of static characteristics showed that taking into account the dependence of the current carrier mobility on the electric field strength, even the dependence $\mu(E)$ that is weak in the quasi-neutral approximation leads to a significant change in the form of the equations that determine the distributions of the current carrier concentration and the electron and hole densities components of the current through the thickness of the base, as well as voltage drops in the structure.

In this regard, the question of the features of static transient processes in semiconductor three-layer structures, in which the base is made of a compensated semiconductor, at high current densities seems to be very relevant.

The purpose of this article is to derive equations that describe the distributions of the concentration and current densities of electrons and holes along the length of the base of injected charge carriers and to analyze the solutions of these equations.

Basic Equations

Let us first consider three-layer structures of the p^+-n-n^+, p^+-n-p^+, n^+-n-n^+, p^+-p-n^+, p^+-p-p^+, n^+-p-n^+ types, through which a current flows with a given density $(\rho = 7.5\Omega\, cm, N_D \approx 6\cdot 10^{14}\ cm^{-3})$, where $\Delta\nu_x(cm^{-1}) = \left(\frac{1}{\lambda_0(nm)} - \frac{1}{\lambda_x(nm)}\right)\times\frac{10^7}{cm}$ are densities of total current, electron and hole currents. We assume that the right, for example, p^+-n and left, for example, $n-n^+$ – transitions of the structure are located at the points $x = 0$ and $x = d$, respectively.

In the simplest case, the charge carrier transport equations have the form:

$$J_n = \left[ep\mu_n(n+n_0)E - eD_n\frac{dn}{dx}\right]\left(1+\frac{E}{E_0}\right), \qquad (1)$$

$$J_p = \left[ep\mu_p(p+p_0)E - eD_p\frac{dp}{dx}\right]\left(1+\frac{E}{E_0}\right), \qquad (2)$$

where $p(p_0)$ and $n(n_0)$ are non-equilibrium (equilibrium) concentrations of electrons and holes. Here, we took into account that the dependences of the mobility $\mu_i(E)$ and diffusion coefficient $D_i(E)$ on the strength of a weak external electric field $(\vec{E})$ are described as $\mu_i(E) = \mu_{io}\left(1+\frac{E}{E_0}\right)$, $D_i(E) = D_{io}\left(1+\frac{E}{E_0}\right)$ [9], where, E_0 is a negative value that has units of measurement of the electric field strength. Then from (1, 2), it is easy to obtain expressions for the electric field strength as

$$E = \frac{jE_0}{e\mu_p\left[(p+p_0)+b(n+n_0)\right]E_0 - j} - \frac{eD_p\left(b\frac{\partial n}{\partial p}-1\right)E_0}{e\mu_p\left[(p+p_0)+b(n+n_0)\right]E_0 - j}\frac{dp}{dx}$$

or

$$E = \frac{j}{e\mu_p\left[p+p_0+b(n+n_0)+N_k\right]} - \frac{D_\rho}{\mu_p}\frac{b-\frac{\partial p}{\partial n}}{\left[p+p_0+b(n+n_0)+N_k\right]}\frac{dn}{dx}, \qquad (3)$$

where $N_k = \frac{j}{e\mu_p E_0}$, b is the ratio of the mobility of electrons and holes.

Substituting (3) into (1) gives expressions for the electron current density, i.e.

$$j_n = \frac{e\mu_n(n+n_0)E_0\cdot j}{e\mu_p\left[p+p_0+b(n+n_0)\right]E_0 + j} + \frac{e^2D_n\mu_p\left[p+p_0+\frac{\partial p}{\partial n}(n+n_0)\right]E_0 + e^2D_n\mu_p j}{e\mu_p\left[p+p_0+b(n+n_0)\right]E_0 + j}\frac{dn}{dx}$$

or

$$j_n^{(x)} = \frac{b(n+n_0)j}{p+p_0+b(n+n_0)+N_k} + eD_n\frac{p+p_0+(n+n_0)\frac{\partial p}{\partial n}+N_k}{p+p_0+b(n+n_0)+N_k}\frac{dn}{dx}, \qquad (4)$$

If we take into account the following expression for $\frac{1}{e}\cdot\frac{\partial j_n}{\partial x}=-\frac{n-n_0}{\tau_n}$ (τ_n is electron lifetime), then we have an equation for the electron concentration in the form

$$\gamma_n\cdot\frac{d^2n}{dx^2}+\tilde{D}_n\cdot\left(\frac{dn}{dx}\right)^2+\alpha_n\frac{dn}{dx}=\frac{n-n_0}{\tau_n}, \qquad (5)$$

and for the distribution of the electron current density:

$$L_n^2\frac{p+p_0+b(n+n_0)\frac{\partial p}{\partial x}+N_k}{p+p_0+b(n+n_0)+N_k}\frac{d^2 j_n}{dx^2}- \\ -j_n+\frac{bnj}{p+p_0+b(n+n_0)+N_k}=0, \qquad (6)$$

where

$$\alpha_n=\frac{b}{e}\cdot j\frac{\left[p+p_0+b(n+n_0)+N_k\right]-(n+n_0)\left(b+\frac{\partial p}{\partial x}\right)}{\left[p+p_0+b(n+n_0)+N_k\right]^2},$$

$$\tilde{D}_n=D_n\frac{p+p_0}{p+p_0+b(n+n_0)+N_k},$$

$$\gamma_n=D_n\frac{\left[p+p_0+b(n+n_0)+N_k\right]\left[(n+n_0)\frac{\partial^2 p}{\partial n^2}+\frac{\partial p}{\partial n}\right]-(n+n_0)\left(\frac{\partial p}{\partial n}\right)^2-b(p+p_0)+bN_k}{\left[p+p_0+b(n+n_0)+N_k\right]^2}.$$

It can be seen from the last relations that equations (5) and (6) cannot be solved analytically. If we consider that there is a linear relationship between the concentrations of electrons and holes, for example, as $n=\theta\delta p$ (see, for example, [10] and the list of literature cited there), then it is easy to obtain an equation for the electron current density in the form

$$\frac{2n+bn_0+\delta\theta(p_0+N_k)L_n^2}{(1+b\delta\theta)n+\delta\theta(p_0+N_k)+b\delta\theta n_0}\cdot\frac{d^2 j_n}{dx^2}- \\ -j_n+\frac{b\delta\theta(n+n_0)j}{(1+b\delta\theta)n+b\delta\theta n_0+\delta\theta(p_0+N_k)}=0$$

or

$$\frac{d^2 j_n}{dx^2}-\frac{j_n-f_2\cdot j}{f_1}=0, \qquad (7)$$

where $\delta=\frac{N_0^0}{N_-^0}$ is the ratio of the concentration of "zero" and "minus" charged impurities, $\theta=\frac{W_{-0}}{W_{0-}}$, $W_{-0}\left(\frac{W_{-0}}{W_{0-}}\right)$ is the probability of transition from the "zero" of the charged impurity to the "minus" of the charged impurity (conversely),

$$f_2=\frac{b\delta\theta(n+n_0)}{(1+b\delta\theta)n+b\delta\theta n_0+\delta\theta(p_0+N_k)},$$

$$f_1=\frac{2n+bn_0+\delta\theta(p_0+N_k)L_n^2}{(1+b\delta\theta)n+\delta\theta(p_0+N_k)+b\delta\theta n_0}. \qquad (8)$$

Thus, (7) is analytically solved both for $n\gg n_0$ and for $n\ll n_0$, i.e., both at high and low injection levels, where the values of f_1 and f_2 become constant. Then the solution of Eq. (7) under the boundary condition of the form can be rewritten in the form

$$j_n=j\frac{(\gamma_1-f_{21})\cdot sh\frac{d-x}{\sqrt{f_1}}+(\gamma_2-f_{21})\cdot sh\frac{x}{\sqrt{f_1}}}{sh\frac{d}{\sqrt{f_1}}}+f_{21}\cdot j, \qquad (9)$$

where $f_{21}=f_2/f_1$, γ_1 is the fraction of the electron current density in the left (right) transition. Then the distribution of nonequilibrium electrons is determined by the relation

$$n(x)=\frac{jL_n^2}{eD_n\sqrt{f_1}}\cdot \\ \cdot\frac{(\gamma_2-f_2)\cdot ch\frac{x}{\sqrt{f_1}}+(f_1-\gamma_1)\cdot sh\frac{d-x}{\sqrt{f_1}}}{sh\frac{d}{\sqrt{f_1}}}+f_{21}\cdot j. \qquad (10)$$

From the last relations, it is easy to obtain expressions that determine the electron density in transitions as

$$n(0)=\frac{j\cdot L_n^2}{eD_n\sqrt{f_1}}\cdot \\ \cdot\frac{\gamma_2-\gamma_1\cdot ch\frac{d}{\sqrt{f_1}}+f_2\left(ch\frac{d}{\sqrt{f_1}}-1\right)\cdot sh\frac{d-x}{\sqrt{f_1}}}{sh\frac{d}{\sqrt{f_1}}}, \qquad (11)$$

$$n(d)=\frac{j\cdot L_n^2}{eD_n\sqrt{f_1}}\cdot\frac{\gamma_2\cdot ch\frac{d}{\sqrt{f_1}}-\gamma_1+f_2\left(1-ch\frac{d}{\sqrt{f_1}}\right)}{sh\frac{d}{\sqrt{f_1}}}.\qquad(10)$$

Similarly, it is not difficult to determine expressions for the electron current density in junctions.

Calculation of the current-voltage characteristic

The current-voltage characteristic for a given structure is determined by the relationship

$$V=\int_0^d E\cdot dx=V_1+V_2,\qquad(12)$$

where

$$V_1=\frac{kT}{e}\cdot\frac{b\theta\delta-1}{b\theta\delta+1}\ln\frac{n(0)[1+b\theta\delta]+bn_0+p_0+N_k}{n(d)[1+b\theta\delta]+bn_0+p_0+N_k},\qquad(13)$$

$$V_2=\frac{J\sqrt{f_1}}{e\mu_p(b\theta\delta+1)}\cdot I,\qquad(14)$$

$$I=\int_0^d\frac{dx}{c_+e^{\frac{x}{\sqrt{f_1}}}+c\_e^{-\frac{x}{\sqrt{f_1}}}+c'},\ C'=\frac{p_0+bn_0-N_k}{b\aleph+1},$$

$$C_\pm=\frac{J\cdot L_n^2\left[\gamma_2-f_1+(\gamma_2-f_1)e^{\pm\frac{d}{\sqrt{f_1}}}\right]}{eD_n2sh\frac{d}{\sqrt{f_1}}},$$

γ_2 is the fraction of the electron current density in the right transition ($x=d$). The calculations took into account the dependence of the concentration of injected electrons in the base of the three-layer structure on the coefficient γ_2, i.e.

$$n(x)=\frac{J\cdot L_n^2}{eD_n\sqrt{f_1}}\frac{(\gamma_2-f_2)\left(e^{\frac{x}{\sqrt{f_1}}}+e^{-\frac{x}{\sqrt{f_1}}}\right)+(\gamma_2-f_1)\left(e^{\frac{d-x}{\sqrt{f_1}}}+e^{-\frac{d-x}{\sqrt{f_1}}}\right)}{sh\frac{d}{\sqrt{f_1}}}\qquad(15)$$

In conclusion, we note that the discussion of our theoretical results on specific three-layer semiconductor structures in a diode inclusion requires separate consideration.

References:

1. Taylor J. D. (Ed.). Ultra-wideband radar technology. CRC press. 2000.
2. Rodin P., Ebert U., Hundsdorfer W., & Grekhov I. Tunnelling-assisted impact ionization fronts in semiconductors. Journal of applied physics,– 92(2). 2002.– P. 958–964.
3. Omar M. A., & Reggiani L. Drift and diffusion of charge carriers in silicon and their empirical relation to the electric field. Solid-state electronics, – 30(7). 1987. – P. 693–697.
4. Vainshtein S. N., Yuferev V. S., & Kostamovaara J. T. Ultrahigh field multiple Gunn domains as the physical reason for superfast (picosecond range) switching of a bipolar GaAs transistor. Journal of applied physics,– 97(2). 2005.– 024502.
5. Rasulov R. Ya., Madgaziyev A. A., Rayimjonova U., Mamatova M. A., & Muminov I. A. Agency of surface recombination on volt-ampere characteristic of the diode with double injection. European science review,– 11–12. 2019.– P. 70–73.
6. Rasulov R. Ya., Rayimjonova U., Mamatova M. A., Nosirov M. X., & Muminov I. A. To the theory of current-voltage characteristics of the three-layer structure of semiconductors in diode switching. European science review,– 11–12. 2019.– P. 74–76.
7. Mamatova M. A., Rasulov R. Ya. Volt-ampere characteristic of multilayer semiconductor structures.– Fergana. Poligraf Super Servis. 2021.– 178 p. (in Uzbek).

https://doi.org/10.29013/ESR-22-5.6-37-41

Rasulov Vohob Rustamovich,
Associate professor of Fergana State University
Rasulov Rustam Yavkachovich,
Professor of Fergana State University
Mamatova Muhhayyo Adhamovna,
Researcher of Fergana State University
Karimova Mahliyo Nematjon qizi,
Undergradate of Fergana State University
Mirzaakbarov Dilshodjon Dovlatboyevich,
Researcher of Fergana State University

VOLT-AMPERE CHARACTERISTICS OF A THREE-LAYER SEMICONDUCTOR DIODE OF DOUBLE INJECTION

Abstract. Expressions are obtained for the electron current density distribution over the thickness of the base of a three-layer semiconductor double-injection diode made of semiconductors with deep impurity levels, which is associated with an increase in the bipolar drift mobility of current-carrying carriers. Analytical expressions for the voltage – current characteristics of such diodes are obtained. The minimum voltage at the base of the diode is determined.

Keywords: current density, electrons, three-layer semiconductor diode, double injection, semiconductor, bipolar drift mobility, current-voltage characteristic.

The voltage – current characteristic S – type in diodes is observed only when the conductivity of the semiconductor thickness increases with current according to a law stronger than linear. This is due to an increase in: a) the rate of thermal generation of carriers due to the heating of the semiconductor thickness by the flowing current; b) injection coefficient $p-n$ – transition with increasing current; c) carrier mobility in a strong electric field upon scattering by ionized impurities; d) lifetime with increasing carrier concentration (τ -mechanism) [1–6].

In this work, the current density distributions over the base thickness and the voltage – current characteristic of three-layer diodes, the base of which is made of semiconductors with deep impurity levels, is calculated, which is associated with an increase in the bipolar (group) drift mobility of carriers. In diodes, the base thickness of which is much greater than the diffusion length, the distribution of injected carriers, therefore, the influence of the electric field on the distribution of nonequilibrium carriers in the diode base drops sharply with an increase in the injection level, although in pure semiconductors the field does not affect the distribution of current carriers.

For definiteness, a three-layer diode is considered in the work, the base of which is made of silicon with an admixture of gold, since the parameters of this material are most fully studied experimentally [7].

Equation for the distribution of current carriers in the base of the structure

Let us consider a one-dimensional three-layer structure, the base of which is made of gold-compensated silicon, and we assume that the length of the base d significantly exceeds the diffusion lengths of the minority current carriers in it. Then, in the stationary case, the distribution of nonequilibrium current carriers over the thickness of the base is determined using the following equations

$$J_p = e\mu_p(p+p_0)E - eD_p\frac{\partial p}{\partial x}, \quad J_n = e\mu_n(n+n_0)E + D_n\frac{\partial n}{\partial x},$$
$$J = J_n + J_p, \tag{1}$$

$$\frac{1}{e}\frac{dJ_p}{dx} = -\frac{p-p_0}{\tau_p}, \tag{2}$$

where μ_n, μ_p and D_n, D_p are the mobility and diffusion coefficients of electrons and holes, respectively, J, J_n, J_p are the densities of the total, electron and hole current, E is the electric field strength:

$$E = \frac{J}{e\mu_p\left[b(n+n_0)+(p+p_0)\right]} - \frac{kT}{e}\cdot\frac{b\frac{\partial n}{\partial x} - \frac{\partial p}{\partial x}}{\left[b(n+n_0)+(p+p_0)\right]}. \tag{3}$$

Using the Einstein relation and the notation $b = \frac{\mu_0}{\mu_p}$, from equations (1, 2) and relation (3) we express the electric field strength in terms of the concentration of current carriers and, then determining the density of the hole component of the total current, and also substituting the obtained value into equation (3). Having made the following designations $j = \frac{J\cdot L_p}{eD_n\cdot n_0}$, $\varepsilon = \frac{e\cdot L_p E}{kT}$, $\xi = \frac{x}{L_p}$, $y = \frac{p}{n_0}$, $\varepsilon = \frac{n_0}{Nf_0^0}$, we obtain the following relations useful for further calculations

$$E = \frac{b\cdot j}{\left[1+b+\frac{ba}{\varepsilon y+1}\right]y+b} + \frac{1-b-\frac{ab}{(\varepsilon y+1)^2}}{\left[1+b+\frac{ab}{y\cdot\varepsilon+1}\right]\cdot y+b}\cdot\frac{\partial y}{\partial \xi}, \tag{4}$$

$$J_p = \frac{j\cdot y - \left[y\left(2+\frac{a}{(\varepsilon y+1)^2}+\frac{a}{(y\varepsilon+1)}\right)+1\right]\cdot\frac{\partial y}{\partial \xi}}{\left[1+b+\frac{ab}{y\varepsilon+1}\right]y+b}. \tag{5}$$

Thus, the equation for the distribution of minority carriers over the thickness of the base can be written in the following form

$$\eta\cdot y'' + \xi\cdot(y')^2 - j\left[\frac{\varepsilon a y^2+1}{\left[y^2\varepsilon\frac{1+b}{b}+y\left(\frac{1+b}{b}+a\right)+1\right]^2}\right]\cdot y' = y, \tag{6}$$

where

$$\eta = \frac{y\left(2+\frac{a}{y\varepsilon+1}+\frac{a}{(y\varepsilon+1)^2}\right)+1}{y\left(1+b+\frac{ab}{y\varepsilon+1}\right)+b}\cdot b, \tag{7}$$

$$\zeta = b\frac{2(1+\frac{a}{y\varepsilon+1})}{y\left(1+b+\frac{ab}{y\varepsilon+1}\right)+b} - \frac{\varepsilon a y\left(1+\frac{1}{y\varepsilon+1}\right)}{(y\varepsilon+1)^2\left[y\left(1+b+\frac{\tilde{a}b}{y\varepsilon+1}\right)+b\right]} - b\frac{\left[y\left(2+\frac{a}{y\varepsilon+1}+\frac{a}{(y\varepsilon+1)^2}\right)+1\right]\left[\left(1+b+\frac{ab}{y\varepsilon+1}\right)-\frac{ba\varepsilon y}{(y\varepsilon+1)^2}\right]}{\left[y\left(1+b+\frac{ab}{y\varepsilon+1}\right)+b\right]^2}. \tag{8}$$

and

$$\begin{cases} \eta = \dfrac{b\left[2\cdot y(a+1)+1\right]}{y\left[1+b(a+1)\right]+b}, \quad \zeta = \dfrac{b\left[b(1+b)-1\right]}{\left\{y\left[1+b(a+1)\right]+b\right\}^2} & at \quad \varepsilon y \ll 1, \\ \eta = \dfrac{b(2y+1)}{y(1+b)+b}, \quad \zeta = \dfrac{b(b-1)}{\left[y(1+b)+b\right]^2} & at \quad y\varepsilon \gg 1 \end{cases} \tag{9}$$

took into account

$$b\frac{\partial n}{\partial x}-\frac{\partial p}{\partial x}=\left[b-1+\frac{a}{(\varepsilon y+1)^2}\right]\cdot\frac{\partial p}{\partial x},, \quad (10)$$

$$bp\frac{p+N_1}{p+N_2}+p+bn_0+p_0= \\ =n_0\left[y\left(1+b+\frac{ab}{y\varepsilon+1}\right)+b+\frac{p_0}{n_0}\right] \quad (11)$$

Note here that with an increase in the hole concentration, the quantity η (ζ): at $y\ll\frac{Nf_0^0}{(1+|\theta)n_0}$ takes the values $\frac{b(2\theta\delta y+1)}{(1+\theta\delta b)y+b}$ $\left(\frac{b(\theta\delta b-1)}{[(1+\theta\delta b)y+b]^2}\right)$, and at $y\gg\frac{Nf_0^0}{(1+\theta)n_0}$ takes the values $\frac{b(2y+1)}{(1+b)y+b}$ $\left(\frac{b(b-1)}{[(1+b)y+b]^2}\right)$. From wich we get that $1\le\eta<2$, and $\zeta\ll1$ at $y\gg1$ (see, for example, [8]).

Above and below x is given in units of the effective diffusion length of holes $L_p=\sqrt{\frac{D_p}{W_{-0}}}$, and the electric field strength in units of $\frac{kT}{eL_p}$.

Вольтамперная характеристика volt-ampere characteristics

To calculate the voltage – current characteristic, it is necessary to know the electric field strength, which in the case under consideration has the form

$$\tilde{E}=\frac{b\cdot j}{\left[1+b+\frac{b\cdot a}{\varepsilon y+1}\right]y+b}+\frac{1-b-\frac{a\cdot b}{(y\varepsilon+1)^2}}{\left[1+b+\frac{b\cdot a}{y\varepsilon+1}\right]y+b}\cdot y', \quad (12)$$

where $\tilde{E}=\frac{L_P\cdot e\cdot n_0}{kT}E$. Then the voltage drop in the structure is determined by the relation

$$U=\int_0^d Edx=\int_0^d\frac{\beta\cdot j}{\left[1+B+\frac{ba}{y\varepsilon+1}\right]y+B}dx+ \\ +\int_0^d\frac{1-B-\frac{ab}{(y\varepsilon+1)^2}}{\left[1+B+\frac{ab}{y\varepsilon+1}\right]\cdot y+B}y'\cdot dx=U_1+U_2. \quad (13)$$

Here

$$U_1=\frac{1-b(a+1)}{1+b(a+1)}\cdot\ln\frac{y_d+\frac{b}{1+b(a+1)}}{y_0+\frac{b}{1+b(a+1)}}, \quad (14)$$

$$U_2=\int_0^d\frac{2j\cdot b\cdot\frac{1}{1+b(a+1)}}{Ae^{k_2x}+Be^{-k_1x}+\frac{b}{1+b(a+1)}}dx=\frac{2\cdot j\cdot b}{1+b(a+1)}\cdot\int_0^d\frac{dx}{Ae^{k_2x}+Be^{-k_1x}}=$$

$$=\frac{2\cdot j\cdot b}{B[\;]}\left\{\frac{\pi}{k_2+k_1}\cdot\left(\frac{A}{B}\right)^{-\frac{k_1}{k_1+k_2}}\cdot\operatorname{cosec}\frac{\pi\cdot k_2}{k_1+k_2}-\sum_{n=0}^{\infty}(-1)^n\cdot\left(\frac{A}{B}\right)^n\frac{1}{(k_1+k_2)n+k_1}-\sum_{n=0}^{\infty}(-1)^{+n}\cdot\left(\frac{A}{B}\right)^{-n-1}\frac{e^{-[n(k_1+k_2)+k_2]d}}{n(k_1+k_2)+k_2}\right\}$$

or

$$U_2=\frac{\pi\cdot b}{[1+b(a+1)]\cdot b_1}\cdot\frac{\left[\sqrt{j^2+1}-j\right]\cdot e^{\frac{d}{2\sqrt{j^2+1}}}}{\sqrt{j^2+1}}\left[\frac{\sqrt{j^2+1}+j}{\sqrt{j^2+1}-j}\cdot\left[\frac{1-\alpha(a+1)+\frac{b}{yd}}{1+a+\frac{1}{yd}}\right]^{-1}\cdot\frac{\gamma[1+b(a+1)]}{1+a+\frac{1}{y_0}}\right]^{\frac{\sqrt{j^2+1}-j}{2\sqrt{j^2+1}}}\cdot \\ \cdot\operatorname{cosec}\frac{\pi k_2}{2\sqrt{j^2+1}}, \quad (15)$$

where $A=\frac{2B\left(e^{k_2d}-e^{-k_1d}\right)k_2}{[1+B(a+1)]\left(\alpha\cdot e^{k_2d}-b\right)}$, $B=\frac{k_1\left(e^{-k_2d}\alpha-b\right)}{k_2\left(e^{k_2d}\alpha-b\right)}$.

Thus, for k_1d and $k_2d<<1$ it is easy to obtain the following expressions

$$U_2 = \frac{2\cdot b\cdot\pi}{\left[1+b\left(a+1\right)\right]}\cdot\frac{k_1}{k_1+k_2}\cdot$$

$$\cdot\frac{\left(k_1+k_2\right)d}{b_1\left(1+k_2 d\right)-c}\left[\frac{b_1\left(1-k_1 d\right)-c}{b_1\left(1+k_2 d\right)-c}\cdot\frac{k_1}{k_2}\right]^{-\frac{k_1}{k_1+k_2}}\cdot\operatorname{cosec}\frac{\pi k_2}{k_1+k_2}$$

Or

$$U_2 = \frac{2b\cdot\pi\cdot d}{[1+b(a+1)]b_1}\cdot\frac{\sqrt{j^2+1}-j}{1+(j+\sqrt{j^2+1})\,d-\frac{c}{b_1}}\cdot$$

$$\cdot\left[\frac{1+[\sqrt{j^2+1}+j]\,d-\frac{c}{b_1}}{1+[j-\sqrt{j^2+1}+j]\,d-\frac{c}{b_1}}\cdot\frac{\sqrt{j^2+1}+j}{\sqrt{j^2+1}-j}\right]^{\frac{\sqrt{j^2+1}+j}{2\sqrt{j^2+1}}}\cdot \qquad (16)$$

$$\cdot\cos e\,\frac{\pi(\sqrt{j^2+1}+j)}{2\sqrt{j^2+1}}.$$

At $dj << 1$

$$U_2 = \frac{\pi\cdot b\left(1+a+\frac{1}{y_0}\right)}{\left[1+b\left(a+1\right)\right]^2\gamma}\cdot e^{\frac{d}{2}}\cdot$$

$$\cdot\left\{\frac{\gamma\left[1+b\left(a+1\right)\right]\left[1+a+\frac{1}{y_d}\right]}{\left\{1-\alpha\left[1+b\left(a+1\right)+\frac{\beta}{y_d}\right]\right]\left[1+a+\frac{1}{y_0}\right]}\right]^{\frac{1}{2}}, \qquad (17)$$

where $y_L = y(x=L)$. Note that for $e^{-k_1 d}\approx 0$ $b_1 e^{k_2 d} >> c$ and $e^{k_2 d} >> e^{-k_1 d}$ from the last relations can be obtained the results of [8]. But, unfortunately, the last approximation is relatively crude: in particular, for a type structure $p^+ - n - p^+$, it gives the following result, $U_2 = \frac{\pi b\cdot d}{\left[1+b\left(a+1\right)\right]}\cdot\frac{e^{\frac{d}{2}}}{\sqrt{-b_1\cdot c}}$ and it is imaginary. So, when calculating symmetrical structures, for example, $p^+ - n - p^+$, $p^+ - p - p^+$, $n^+ - n - n^+$, $n^+ - p - n^+$ it is not necessary to use the last approximation.

Conclusion

In conclusion, we note that the rate of hole recombination, i.e. the total number of holes captured per unit of volume per unit of time is described by the following expression: $R_p = \left(W_{-0} f_- + W_{0+} f_0\right) p$. We also note the following. At low hole concentrations, the quantities f_- and f_0 in Eqs. (2) and (9) can be replaced by their equilibrium values. In particular, at $n = \theta\delta p$ (9) takes the form $R_p = \left(f_-^0 W_{-0} + f_0^0 W_{0+}\right) p$. At hole concentrations satisfying condition $p > \frac{N}{1+\theta}$, the impurity states of gold are recharged, and now there should be more electrons than holes, just by the amount of the formed uncompensated charge, and the recombination rate will be determined by the corresponding stationary values of the fractions of minus and zero-charged atoms of deep impurities in the equilibrium state. Thus, the difference between the electron and hole concentrations increases from the equilibrium electron concentration to $N\left(\theta f_-^0 - f_0^0\right)$. This means that in this case the nonequilibrium concentration of nonequilibrium electrons can exceed the concentration of equilibrium ones by several orders of magnitude. In this case, the lifetime of holes will change from $\tau_1 = \frac{1}{f_-^0 W_{-0} + f_0^0 W_{0+}}$ to $\tau_2 = \frac{\theta+1}{W_{-0}+\theta W_{0+}}$.

References:

1. Gurin N. T., Korneev I. V., Maksin A. N., Novikov S. G. Position-sensitive combined device with N-shaped voltage – current characteristic // Proceedings of the IV Russian seminar on fiber lasers.– Ulyanovsk: UlGU. 2010.– P. 125. (in Russian).
2. Kashtankin I. A., Turin N. T. Temperature characteristics of bipolar N-devices with a controlled voltage – current characteristic // Nano- and microsystem technology.– No. 6. 2006.– P. 41–43. (in Russian).
3. Adirovich E. I., Karageorgy-Alkalaev P.M., Leiderman A. Yu. Double injection currents in semiconductors.– M.: Soviet Radio, 1978.– 320 p. (in Russian).

4. Stafeev V. I., Vikulin I. M. S-diodes semiconductor devices and their application / Ed. Ya. A. Fedotova.– M.: Sov. Radio.– No. 28. 1974.– P. 28–56. (in Russian).
5. Kazarinov R. F., Skobov V. G. On the theory of nonlinear galvanomagnetic phenomena in semiconductors.– ZhETF,– Vol. 42.– No. 4. 1962.– P. 1047–1053. (in Russian).
6. Stafeev V. I. The influence of the resistance of the thickness of a semi-conductor on the form of the voltage – current characteristic of the diode. ZhTF,– Vol. 28.– No. 8. 1958.– P. 1631–1641. (in Russian).
7. Milns A. Impurities with deep levels in semiconductors.– Moscow, Mir. 1977.
8. Baranenkov A. I., Osipov V. V. Volt-ampere characteristics of long diodes from compensated semiconductors // FTP.– Vol.3.– No. 1. 1969.– P. 39–44. (in Russian).

https://doi.org/10.29013/ESR-22-5.6-42-45

Utamuradova Sharifa Bekmuradovna,
Doctor of Physical and Mathematical Sciences,
director of Research Institute of
semiconductor physics and microelectronics
Naurzalieva Elmira Mahambetyarovna,
PhD student of Research Institute
of semiconductor physics and microelectronics

RAMAN SPECTROSCOPY OF STRUCTURAL DEFECTS RELATED WITH SILVER ATOMS IN SILICON

Abstract. Vibrational and structural properties of silicon doped with silver atoms were investigated using Raman spectroscopy. It has been established that the introduction of silver atoms in silicon increases the interatomic distance in the crystal lattice, which, in turn, shifts the positions of the vibration peak to lower ones.

Keywords: Raman Spectroscopy, silver, interstitial and substitutional defects.

Introduction. It is known that the technological route for the manufacture of almost any semiconductor device is accompanied by various cycles of low- and high- temperature treatments, which inevitably leads to the formation of various kinds of structural defects and impurity centers, as well as to the degradation of device parameters. The degradation of the device parameters based on silicon structures to some extent depends on uncontrolled impurities – oxygen, carbon, metals that are in the silicon wafer or introduced during the manufacture of devices. Of all the contact impurities (Cu, Al, Au, Ag, etc.) – silver is one of the available metals [1].

It is known from theory that the diffusion mechanism allows impurity atoms to be in two states: i) S-substitutional atoms; ii) I-interstitial states (fig. 1). For example, the authors Rollert et al. [2] showed that the overwhelming majority of Ag impurity atoms are present at interstitial sites (Ag_I); and that substitutional silver (Ag_S) either does not occur or occurs only in very low concentrations. Using EPR studies, the authors of [3] identified this isolated Ag, which represents only a small fraction of the total amount of impurity silver atoms present. Today, there is no clear picture of the microscopic structure of defects related with silver atoms in silicon. Thus, the topic of this work is relevant and promising in terms of using its results.

In this paper, the surface states of silver atoms in silicon are considered by Raman spectroscopy.

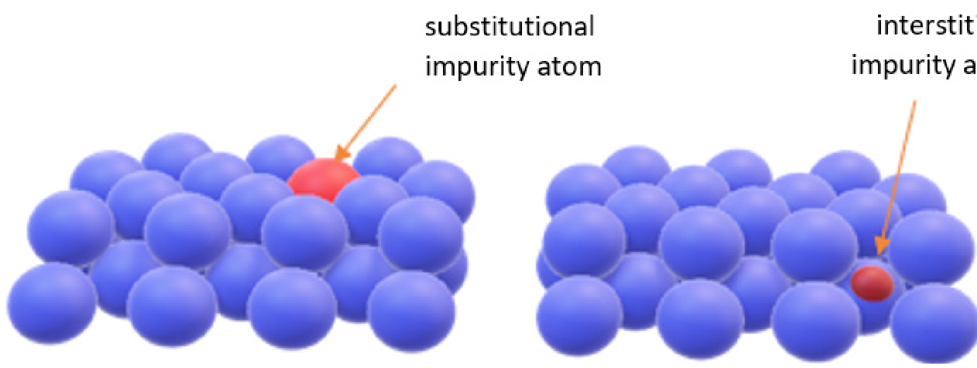

Figure 1. Distribution of impurity atoms in silicon crystal

Experimental technique. Samples of n-type silicon ($\rho = 7.5\Omega\, cm$, $N_D \approx 6 \cdot 10^{14}\ cm^{-3}$) grown by the Czochralski method were selected for measurement. Doping of the silver impurity was carried out by the diffusion method at a temperature of 1200 °C for 2–10 hours. The complete solubility of silver atoms in silicon at this temperature is achieved up to $\sim 6.5 \cdot 10^{15}$ cm^{-3}. Raman spectra were obtained on an Ocean Optics QE65 Pro spectrometer with a 785 nm laser and an integration time of 500 ms.

Raman spectroscopy has proven to be a key experimental technique due to its ability to identify structural and electronic effects in non-destructive measurements. Raman spectroscopy, a fast and convenient method for study of the vibrational and structural properties of materials, is widely used to investigate the structures of crystalline and amorphous silicon semiconductors [4]. Raman scattering can measure changes in vibrational frequencies induced by the microstructure or the presence of local deformations, which can be produced by distortion of the bond angle. In this paper, the surface states of silver and gadolinium atoms in silicon are considered by Raman spectroscopy. Raman spectroscopy studies vibrational energy levels by looking at the energy difference between laser light incident on the sample and the rare photon scattered inelastically via the Raman effect. This energy difference, known as the Raman shift, is reported in energy units called wavenumbers (cm^{-1}).

The following equation shows how to calculate a Raman shift, Δv, in cm^{-1} using the laser wavelength (λ_0) and a Raman peak wavelength (λ_x) in nm:

$$\Delta v_x (cm^{-1}) = \left(\frac{1}{\lambda_0 (nm)} - \frac{1}{\lambda_x (nm)} \right) \times \frac{10^7}{cm}$$

Results and its discussion. The Raman spectra of the light of the initial sample Si<P> and doped with silver atoms Si<Ag> are shown in (fig. 2. and fig. 3).

The Raman spectrum of Si exhibits a high peak in the region 519–521 cm^{-1} with a FWHM of 8–12 cm^{-1}. Intensity of first-order scattering due to optical phonons (TO, LO) at the central point Γ of the Brillouin zone.

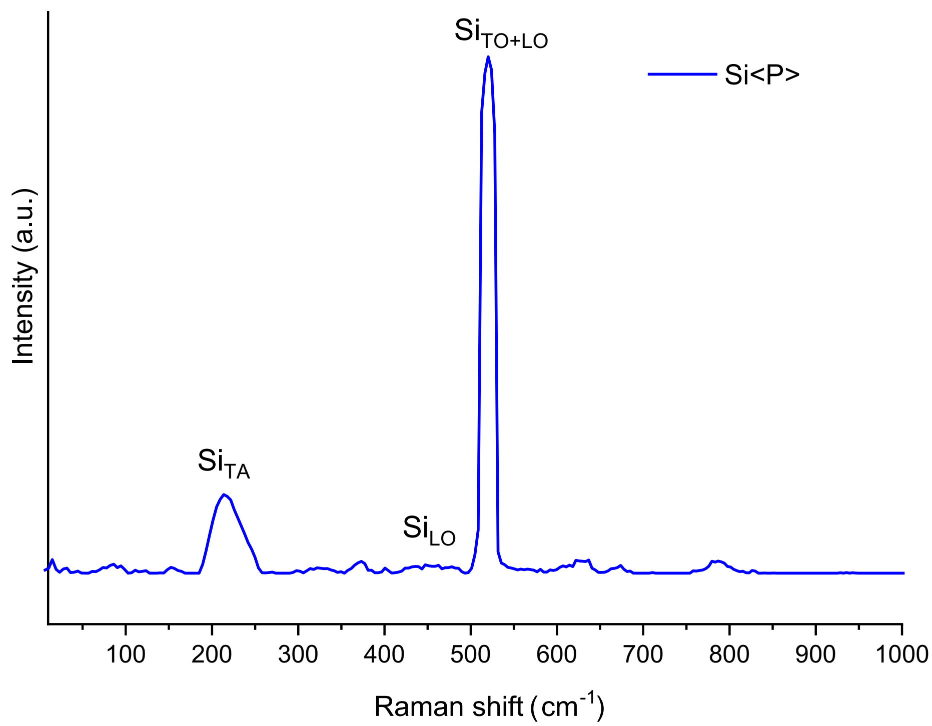

Figure 2. Raman shift of initial silicon. Modes: Si$_{TA}$ – 215 cm^{-1}, Si$_{LO}$ – 412÷494 cm^{-1}, Si$_{TO+LO}$ – 521 cm^{-1}

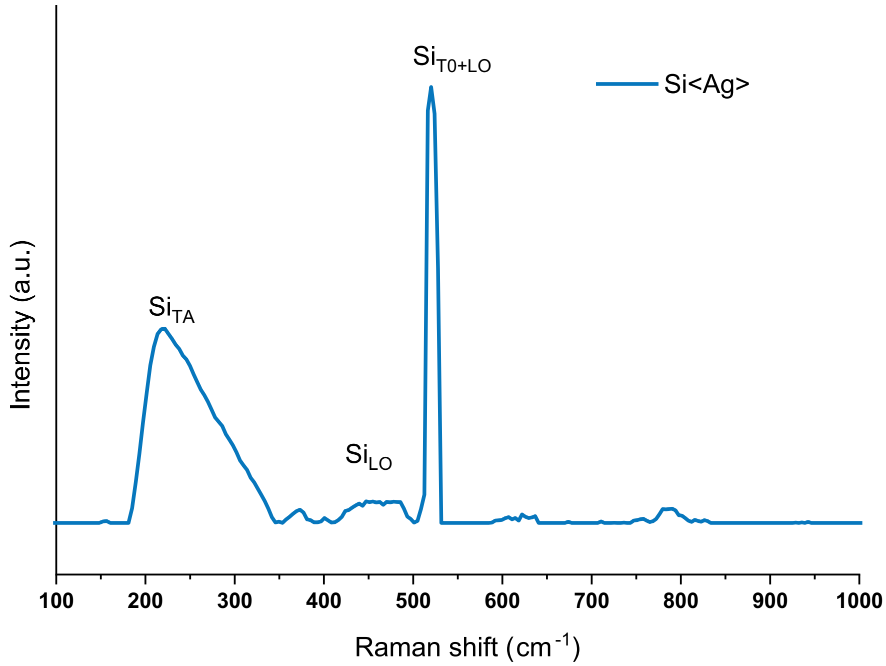

Figure 3. Raman shift of silicon doped with silver atoms. Modes: Si_{TA} – 221 cm^{-1}, Si_{LO} – 414÷504 cm^{-1}, Si_{TO+LO} – 520 cm^{-1}

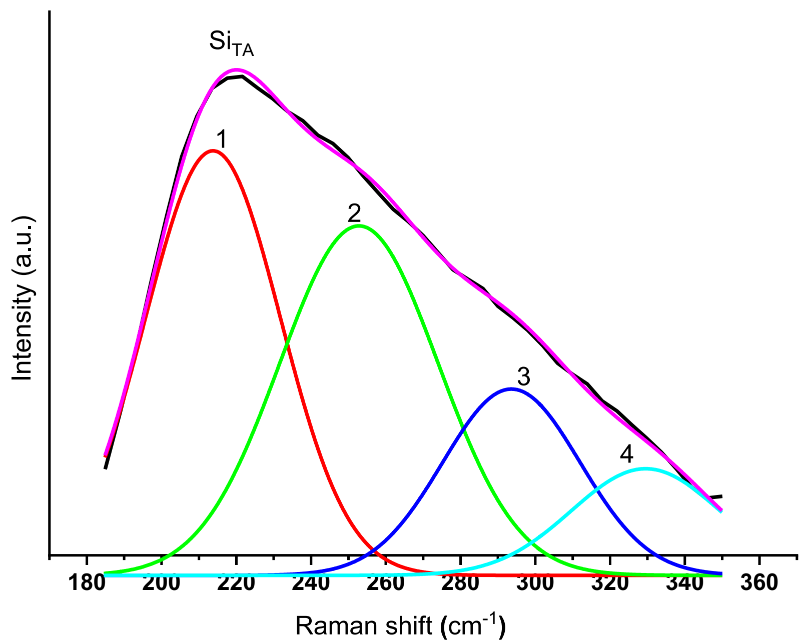

Figure 4. Gauss distribution of acoustic mode (TA) of Si<Ag> sample: 1–214cm^{-1}, 2–253 cm^{-1}, 3–294 cm^{-1}, 4–330 cm^{1}

In contrast to the main peak, one can observe scattering by acoustic phonons at 221 cm^{-1} (2TA). The authors of [5] attribute such oscillations to the intrinsic Si interstitial defect. As can be seen from the fig.3, further doping of n-Si single crystals with silver impurity atoms leads to some change in the Raman spectra. When comparing the Raman spectra of the Si<P> and n-Si<Ag> samples, it can be seen that after doping with Ag atoms, some of the silicon atoms (Si_s) leave the crystal sites, which leads to a slight decrease in the intensity of the fundamental vibration (TO) at 520 cm^{-1}.

Compared to the acoustic phonon peak of the second order of the Si<P> sample at 221 cm^{-1}, which describes the interstitial nature of the crystal [5], the corresponding Raman peak in the Si<Ag> sample has an increased intensity, its line width is broadened, and the line shape becomes asymmetric with a small tail on the low energy side extending to 346 cm^{-1} (Fig. 3). The Gaussian distribution of this peak showed several scattering peaks at 214, 253, 294, 330 cm^{-1}, which is shown in (fig. 3). Analyzing the results of many publications [2; 5], this modification can be explained by an increase in the concentration of interstitial defects (Si_I, Ag_I, SiO_2, etc.) after silver doping in silicon, which is caused by an increase in the intensity of the 221 cm^{-1} peak.

Conclusion. Thus, the processes of Raman scattering of light in silicon doped by diffusion with silver impurities have been studied. It has been shown that an increase in the concentration of interstitial defects in silicon doped with silver atoms leads to an increase in the intensity of the 221 cm^{-1} peak. It was also found that in this mode at 221 cm^{-1} have four components with Raman shift at 214, 253, 294, 330 cm^{-1} which can form nanodefects with self-interstitial impurities of silicon.

References:

1. Vincent T. M. and Estreicher S. K.J. Appl. Phys.– 128. 2020.– 155703 p. URL: https://doi.org/10.1063/5.0026161
2. Rollert F., Stolwijk N. A. and Mehrer H., J. Phgs.– D20. 1987.– 1148 p.
3. Son N. T., Kustov V. E., Gregorkiewicz T. and Ammerlaan C-A-J-, J. Appt. Phgs.– 73. 1993.– 1797 p.
4. Rong-ping Wang, Guang-wen Zhou, Yu-long Liu, et. al. “Raman spectral study of silicon nanowires: High-order scattering and phonon confinement effects”. Phys. Rev. B,– 61 (24). 2000.– P. 16827–16832. URL: https://doi.org/10.1103/PhysRevB.61.16827
5. Xiao Dong, Xiuxiu Fang, Yongyong Wang, and Xiaohui Song. “Raman spectra and optical properties of the chalcogen-hyperdoped silicon: a first-principles study”. Opt. Express – 26. 2018.– A796-A805.

Section 5. Chemistry

https://doi.org/10.29013/ESR-22-5.6-46-58

Bulutoglu Efe,
Istanbul, Turkey

SPRAY DRIED FRUIT POWDER USING FRUIT JUICE CONCENTRATES

Abstract. The process of spray drying is regarded as a method that conventionally converts fruit juices like orange juices or concentrates to the powder fruit form. In this process, three main processes are involved in spray drying (Murungesan et al. [29]). These processes are:

- Atomization
- Droplet –hot air contact and evaporation of moisture.
- Separation of products that have dried from the exit air

Feed

- Orange concentrates and lemon concentrates with water (slurry mixture)

Output

- Orange fruit powder
- Lemon fruit powder

In this study's scope, we investigated the procedures within the fruit drying spray responsible for yielding fruit powders using orange and lemon fruit concentrates. The production of fruit powder from fruit condenses calls for the use of drying aids, which function as an agent for reducing stickiness concerns that arise during the fruit spray drying technique. This paper illustrates the process of fruit spray drying with orange and lemon fruit concentrates and how the fruit powder form can be used in a production application (Boonyai et al. [35]).

The concentrated orange and lemon juice are spray-dried using air that is dehumidified as a medium for drying, and the agent used for drying is maltodextrin. For the spray drying process, the piloting-scale dryer is used.

Keywords: spray drying, fruit powders, fruit concentrates, processing of lemon and orange juices

Introduction

A spray drying process is an operational unit such that liquid products (orange and lemon fruit concentrates) go through the process of atomization in a stream of hot gas in order to get instant fruit powder. The fruit spray drying method is developed in relation to the production of dried fruit powders. The initial solution (slurry) used as a feed in the spray drying activity can be in a solution form that is a suspension emulsion (Gharssallaoui et al. [2]). The product is turned into powder, granules, and agglomerates. These forms depend on chemical features, the feed's physical feature, the feed and the design of the dryer, and how it is operated (Filkova et al., [4]). The requirements of the spray dry, such as the drying agent concentration that is used, the temperature of the inlet, the flowing rate of the feed, and the features of the feed, all affect the fruits that are spray dried as well as the characteristics of the pulp powder that is produced during the process (Chegini et al. [8]). The different ways the spray dryer displays itself include concurrent, counter current and flow with the mixture. Spray dryers that are concurrent are commonly used. In concurrent, there is the travel of the droplets of the feed-in in a direction that is the same as the flow of the gas used for drying (Zbincinski et al., 2002).

Steps for spray drying process

Atomization Step

This is among the essential steps in the fruit spray drying activity; this process enhances the conversion of fluid fruit into tiny droplets (Murungesan et al., [18]). Due to the reduction in particle size and particle dispersion in the gas used for drying, an exponential increment of the particle area is subsequently done, enhancing feed drying quickly. When the droplet size is tiny, and the feed fluid distribution is minimal, there is moisture in the material without the material's integrity being affected. Because the droplet size is small, atomization is performed by atomizers, commonly classed as rotary sprayers, pressure nozzles, compressor nozzles, and supersonic nozzles. The choice of atomizers is determined by the specific feed selected to be dried, the ultimate qualities of the intended feed, and the particle shape.

In this case, we chose the orange and lemon concentrates to be used as the feed-in fruit spray drying.

Droplet-air contact and Evaporation of Moisture

Generally, the air of the atmosphere is used to dry in the spray drying process. During the spray drying activity, the air from the atmosphere undergoes the process of filtration through the system used for filtering. Then it is preheated subsequence per the parameters of opera ration. At times, nitrogen gas and other inert gases are used with the dependence on the feed undergoing the drying process and the instability and sensitivity of the feed concerning oxygen (Sollohub and Cal [25]). The process of the feed droplets being dried after contact with the medium for drying in the spray drying activity is the effect of simultaneous heat and the transfer of mass. The drying medium heat is transferred to the droplets through the convection method, and then the conversion of the heat latent during the process of evaporating the moisture content of the droplet. The heart rate and heat transfer depend on the droplet's diameter, relative velocity, and air velocity (Orsat and Mungesan [29]). The starting time for drying in the spray drying process starts once there is contact between the droplet and the medium for drying. This process is accompanied by the rate of a falling duration, where the drying rate starts decreasing, and the time ends immediately when the droplets can reach the critical moisture content (Filkova et al. [4]).

Separation of the substance that is dried from the exit air

The cyclone, which is positioned outside the dryer and serves the purpose of reducing the amount of product lost to the environment, is used in the separation process. The denser particles are regained at the drying chamber's base, while the finer particles are passed via the cyclone to undergo separation from the humidified exit air (Gharsallaouii et al. [4]).

The types of fruit powders that can be made from the orange and lemon concentrate

The lemon and orange concentrates can be spray dried to create fruit powder. These fruit concentrates are typically pasteurized; mixing with the carriers takes place to ensure that they are stably dry for them to be fed to the spray drying machine. The mixture usually undergoes a pumping process through the nozzle and then passes into the chamber that has been heated with the hot air vortex. As a result, the water in the mixture is evaporated then the fruit powder is collected at the outlet. The following are some fruit powders that can be formed from the orange and lemon juice concentrate depending on the manufacturing feasibility, cost, and the final product quality required (Boonyai et al. [35]).

Roller fruit powder/belt dried fruit powder

This type of fruit powder is commonly primary. For this type of powder to be achieved, there is a long set of rollers in which fruits are passed through a chamber that has been heated in the roller drier or passed into a long belt conveyor through a chamber that is heated. The higher temperature in the chambers can remove as much water as possible from the fruits, and then the fruits that have been dehydrated are then milled, ground, and then crushed into the powder form that is fine.

It allows specific formulations. – These are relations to the properties of the powder, texture, and flavors. This process is also favorable for drying in an atmosphere with less oxygen because it avoids oxidation.

Disadvantages of roller fruit powder process.

The drum drying is limited to the liquids that are highly viscous or pastes. Therefore, this process is only suitable for specific product types.

Vacuum dried fruit powder.

The way is a specialized process of producing the fruit powder, and in this case, there is avoidance of high temperature (Murungesan et al. [18]). The fruits are dried just like the roller fruit powder, but the batch process is sealed in the vacuum chamber. The vacuum drops the boiling point of water to 30 degrees by illustrating that the fruits require low temperatures for water to be evaporated from the fruits. This process is suitable for fruits that are sensitively suited to temperature even though the process is expensive; it is minimally harsh on the fruits, preserving the flavor of the fruit powder.

Advantages of vacuum fruit powder process.

It lengthens the storage time of the fruit powders while their original flavor is maintained.

The vacuum-manufactured fruit powders do not change color and do not develop foul odors (Murungesan et al. [18]).

This process can enable a wide variety of new products throughout the year, even during the off-season of used fruit.

This process also enhances the prevention of unnecessary wastage of fruit powders.

A vacuum dryer provides a large surface for transferring heat throughout the body; therefore, there is faster drying action.

There is supplied hot water to the dryer that facilitates the process of drying at the temperature that is desired.

The electrically-heated hollow shelves are used.

The handling of materials in this process is effortless.

Disadvantages of vacuum-dried fruit powder process.

The dryer is a type of process based on a batch.

The efficiency of the process is low.

The process is costly.

The cost of labor in this process is high.

The process needs to be highly maintained.

The process can be subjected to the danger of overheating because of the vacuum.

I have freeze-dried fruit powder.

The process of freeze-drying is a batch process that occurs in a sealed chamber. Freezing of the fruits is done, and then there is a gradual reduction in the pressure, which makes the water in the fruit directly jump from the phase of ice straight to the phase of vapor. This process can be classified as a sublimation process. The water flavor in the fruit leaves freely from the fruit. This process highly results in hydrated fruit with fully maintained integrity. After this is done, the fruit can be milled and crushed into the required powder. Because this process is expensive, it results in desired results, producing highly priceable fruit powder, arguably the most preserved (Murungesan et al. [29]).

Advantages of freeze-drying

The fruit powders produced through this process have nutritional value and are synthetically free from artificial and highly processed materials.

The fruit powders from this process are close to their new form. This means that when the fruit-dried powders have retained their nutritional values, they support the desire of the consumer's nutrition from the whole fruit.

Customization advantage

This means that the fruit powders from the process mentioned earlier can customize the project goals and the unique needs.

Application in varieties

The capabilities of blending and customization allow the fruit processors to incorporate orange and lemon fruits into different large varieties of applications.

I have a prolonged shelf life. -The shelf life of any fruit powder depends on the moisture content of the fruit concentrates. Bacterial growth is potentially removed when water is removed from the fruit powder. The fruit powder's moisture differs from different fruits, but the average content of the fruit powder's moisture is about 3%. The average shelf life of a fruit powder that has been freeze-dried depends on the packaging of the fruit powders, the storage temperature, and the fruit powder production fruit.

Disadvantages of freeze-drying fruit powder

There is a requirement for water to reconstitute the process.

The process is slow and has an average cycle of 24+ hours.

There is a dislike for the dry and Styrofoam texture of the fruit powders produced through this process.

Air-tight containers are required for a longer time of storage.

There is no space saving because the fruit's cellular structure is mostly retained.

Regular dehydration of the fruit powders is better.

It has a high fruit powder production cost.

Spray Dryer Parameters

Natural hygroscopes and property of thermoplasticity of the fruit juice is the most common issue in transporting and handling the powdered juice fruit produced from the fruit dryer. The pilot plant test is usually used for the performance specification to be met. Examples of these specifications are: the conditions used in optimization, flow current of the type of the dryer, time residence, air humidity, and the ancillary equipment (Adhikari and Bhabdari [5]).

These specifications are required to complete the drying process without influencing the fruit powder's quality. It also prevents the formation of unacceptable wall deposits on the semi-dried product. The spray dryer used in the industrial orange and lemon fruit drying to produce the fruit powders should be designed using information that is accurate according to the behavior of the agent used for dying. The above specification should be analyzed through a laboratory test of the spray dryer.

Two complicated challenges arise during the production of orange and lemon fruit powders. There are two significant problems to be solved: one is the powder's stickiness and its difficulty in handling, and the other is caused by the features of the citrus concentrates that impact the manufacturing of the powdered orange and lemon fruit (Boonyai et al. [35]). For the hygroscopic decrease of citrus fruit juice, drying agents are needed. It is possible to speed up the drying process by modifying the physical characteristics of the materials employed as drying agents. Maltodextrin is one of the finest drying agents for manufacturing fruit powders utilizing orange and lemon concentrates. Other drying agents include corn syrup, natural gum, sucrose, and others. The dryer's walls don't attach to the particles while using these drying ingredients, which boosts power generation.

When fruit powder production using orange and lemon concentrate is not done using the drying materials, there is a limited production of the fruit powders. Therefore, in addition to the production of powder, the fruit spray dryer's qualities depend on the operation variables.

The optimum operating conditions are obtained when the operating variables are studied and determined in producing fruit powders using the orange and lemon concentrates.

The following results were obtained in the test for the drying without additive material and for drying using the agent drying materials.

Drying without the addition of drying agents

The design factors include the flow of air current, condition operation of the dryer, orange and lemon juice characteristics, time of residence, the drying agent suitable for the process, and temperature of the point of stickiness (Boonyai et al. [35]). The airflow currents suitable for fruit drying, in this case, are concurrent due to the low heat damage. For undamaged concentrates and the viscosity of orange and lemon juice to be suitable, the feed's maximum temperature should be around 60 degrees Celsius. The temperature for atomization should be very hard at a less temperature of 5 degrees Celsius. The most suitable feed concentrate temperature for the orange and lemon concentrates should be between 20–35 degrees Celsius. When the orange and lemon fruit juice concentrates were produced without drying agent materials, there was no production of the orange and the lemon fruit powder. The feed materials get stacked on the dryer's walls and the cyclone. As the process continued, a hard film of glass was shaped on the wall. During the changing of the conditions for operating, like the change in the inlet air temperature and the rate of feed flow, there was yield in the powder but no improvement (Adhikari and Bhabdari [5]).

When drying agent materials like sucrose and fructose are used, the orange and lemon fruit concentrate the hygroscopic nature and thermoplastic nature, so the fruit dried powder and the particles that have been dehydrated do not stick on the walls of the dryer.

When the orange and lemon have irregular structures, water can act as a plasticizer and enhance the chaining of the irregular structure of the lemon and orange materials. The little water applied enhances the reduction of the transition temperature of the glass until it reduces to temperatures below the home temperature.

Drying through the use of agent drying materials

When the experiments are conducted using the maltodextrin dying agent in the orange and lemon concentrates, the yield of the powders increases. When the conditions of the operating dryer are measured, the results show that the yield of the fruit juice powders increased from 18–35 percent, and deposition on the wall still occurred in the range of 67–82 percent. The cyclone and chamber particles accumulated, and the physical powder properties are measured. The density and bulkiness of the powder showed a decrease (Murungesan et al. [29]).

Time of Residence- the residence time is sufficiently required to facilitate the necessary permission to complete the drying process. The spray dryer residence time is essential in drying to prevent the under-sizing and over-sizing of the chamber used for the drying process.

The temperature of the sticky point – The temperature at which the amount of soft powder put on the plate sticks on the wall of the plate.

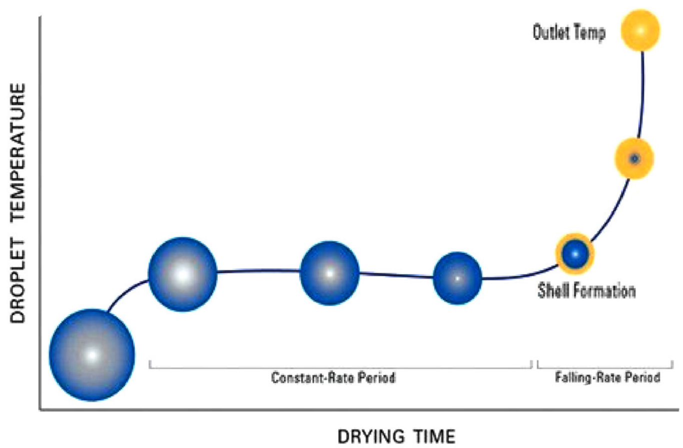

Figure 1. Lewandowski et al., 2019

Spray drying of lemon and orange juice concentrates

In the drying technique, the spray drying process is applicable in producing the fruit juice powder. In fruit juice spray drying, this process is essential because it aids in handling the demand in the market through the years. When there is the presence of high content of moisture in the orange and lemon concentrates, there will be a high activity of water in the feed that will cause a loss of fruit quality that leads to increased enzymatic activities and growth of micro bacteria. As a result, the reduction of water content in the feed materials, which is **the slurry mixture**, and the activities of water in lemon and orange concentrates lead to the production of the desired quality dried fruit powder. **When the feed slurry mixture** consists of fruit concentrate and water used to produce fruit dried powder, the fruits used as concentrates can be divided into two main groups. These include the sticky and non-sticky groups.

The non-stick fruits are easily spray dried through a designed simple dryer, and the powder that is finally produced remains flowing freely (Tan et al. [24]). When the fruit is sticky, issues arise in the process of drying when using the standard conditions. The sticking fruits get stacked on the walls of the dryer, or they generally undergo agglomeration in the chamber used for drying. This leads to the conferment of the systems to the problems with the operation and production of low-quality powder products. Consider the diagram below.

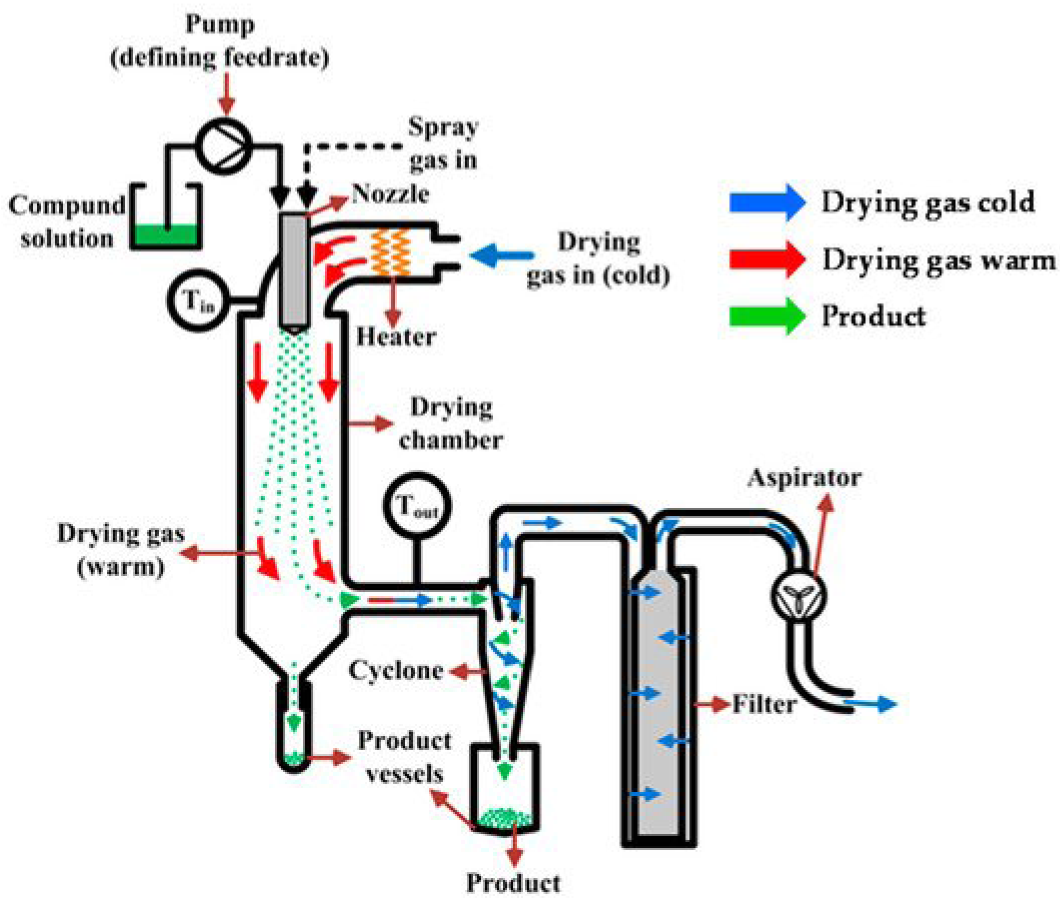

Figure 2. Buchi Labortechnik AG, 2019

The cohesion and adhesion characteristics of the powder's stickiness are illustrated in the form of stickiness between the particle-particle and the particle's stickiness on the dryer's surfaces (Bahu et al. [6]). The measure at which the forces hold the particles together to their internal property is cohesion which causes the lump to form in the bed powder. Therefore, the forces needed for the powder's agglomerates to be broken must be larger than the force of cohesion (Mani et al. [28]).

The force of adhesion has interfacial features, which is the tendency of particle powder to attach to the surfaces of the spray dryer used for drying. The cohesion and adhesion forces are designed as critical factors of spray drying dryers and drying process conditions. The stickiness associated with the spray drying technique can both be present during the spray drying of sugar-rich fruits. In this scenario, the spray-dried powders are made from orange juice concentrates, and orange juices, by definition, include some sugar. As a result, when performing fruit spray drying of orange juice concentrates, expect both stuckness and stickiness to occur (Adhikari and Bhabdari [5]).

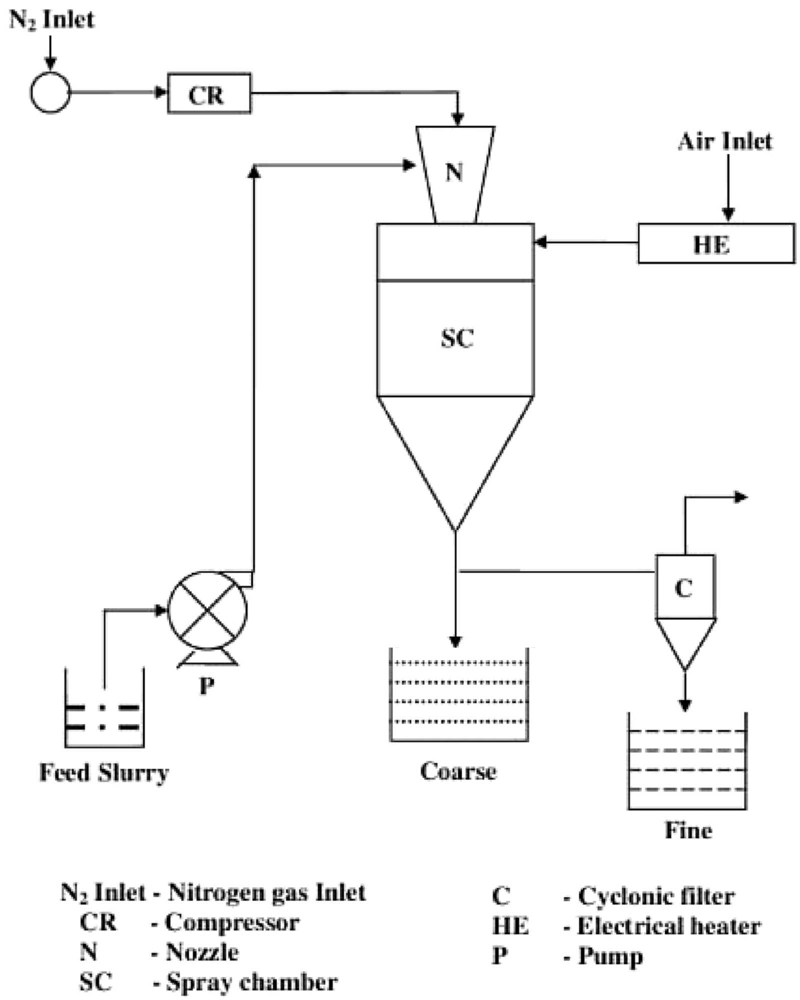

Figure 3. Flow diagrams for the process of fruit spray drying using lemon and orange fruit concentrates

The stickiness that occurs due to antiparticle is cohesion and is brought by the formation of immobile liquid bridges, the intermolecular forces caused by the interlocking mechanical forces and forces of electrostatic and bridges of solids (Boonyai et al. [35]). The adhesion of particle powders with the wall chambers of the dyer is one of the most causative factors for the loss of materials in the process of fruit drying of the sugar-rich fruits and acid-rich fruits. Then the powder quality is decreased when retaining on the dryer walls occurs for a long time (Maa et al. [37]). In this case, we are using the orange and lemon, which are sugar-rich and acid-rich materials.

The process of spray drying orange juice and lemon juice, since they are sugar and acid-rich materials, has witnessed some difficulties due to their lower molecular weights of the sugars and organic acids. The high hygroscopic nature, thermoplasticity, and low temperature of glass are the features that lead to the powders' stickiness on the dryer's wall.

At a temperature used for spray drying T_g+ 20 degrees Celsius, the components can form soft particles, with the surfaces being sticky, leading to the stickiness of the powder and the formation of paste structures rather than powder forms (Jing et al. [16]). The molecules have high molecular mobility due to the molecule's low transition glass temperatures, leading to the problem of stickiness and the prevailing average temperatures in the dryer.

The temperature of the glass transition parameter is the most essential and suitable parameter used in assessing the lemon fruit juice and orange fruit juice materials used in spray drying (Langrish et al. [32]). To minimize the thickness problem in spraying drying, drying agent materials with high molecular weights are used in the feed materials before atomization takes place to ensure increased glass transition temperatures (Cabral et al. [1]).

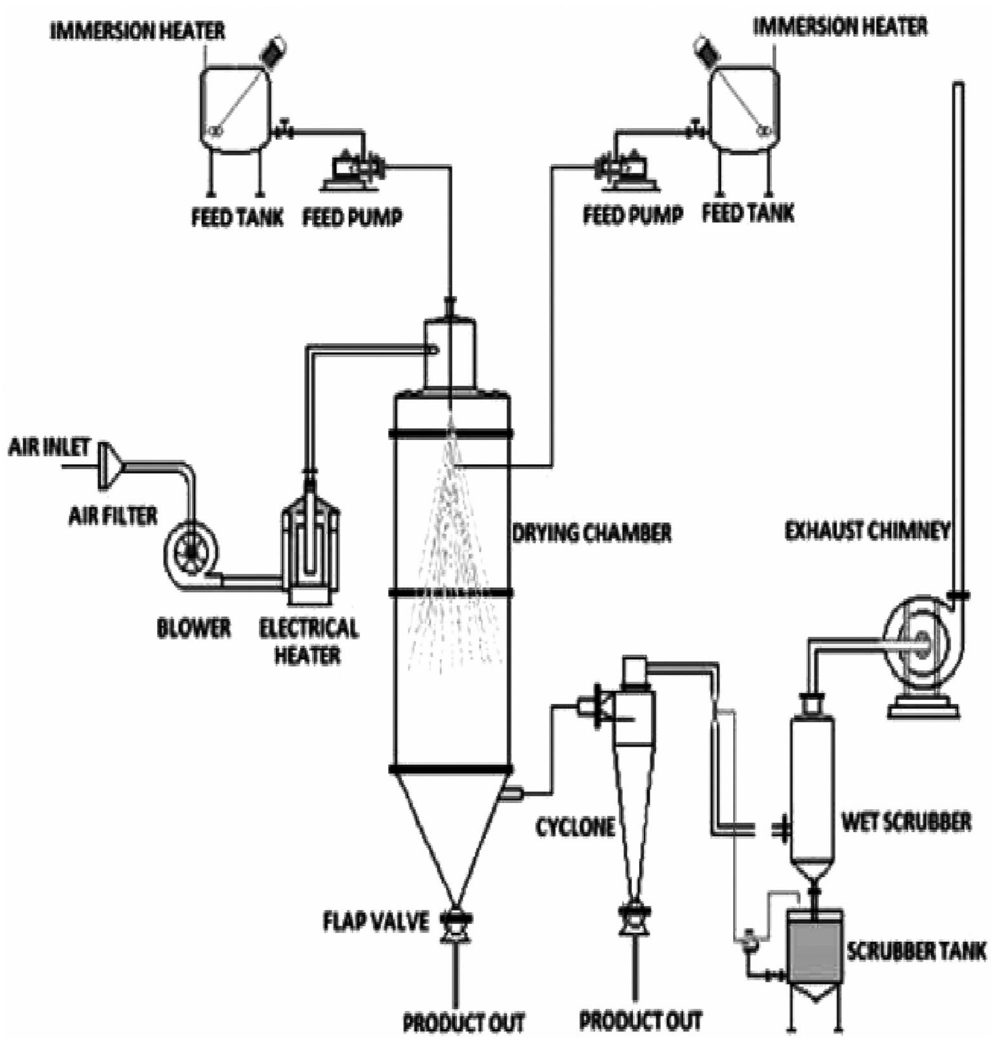

Figure 4.
Sourced from (Bhandari, Data, and Howes, 1997)

The drying agent materials are different like maltodextrin, Arabic gum, starches that are modified, and proteins applied in the process of spray drying to ensure minimization of the stickiness of the powder that occurs in the walls of the dryer (Caliskan and Drum [21]). The maltodextrin product consists of starch that has been hydrolyzed and entailing the D-glucose units linked by (1→4) glycosidic bonds. Maltodextrin is described using its equivalence of dextrose (D. E.), which is averagely related to the inverse of the molecular weight. Maltodextrin is considered because its cost is low, and it is helpful in fruit drying using a spray dryer. At the same time, Gum Arabic is an exudate of the acacia tree, obtained from the natural plant. Moreover, it consists of structures that are highly ramified in hetero-polysaccharide. The Arabic gum is the only gum that can be used in fruit juice products with high solubility and low viscosities in an aqueous solution. As a result, the spray drying process is made more accessible (Bemiller and Whistler [28]). Due to the increased overall value of T_G in the feed concentrates, powder stickiness is decreased by using maltodextrin, Arabic gum, and starches modified as materials used for dying during the spray drying process. When proteins are used as drying agent materials, they help minimize the stickiness problem through the property's modification of the surface of the droplets and particles that have been atomized while considering the forming of film features and protein surface activities (Adhikari et al. [26]). Due to the forming of film feature and surface activities of the protein, there is the migration of proteins to the surface of the air-water interface of particles that have undergone atomization of feed droplets hence the formation of a film protein which undergoes conversion into skin glass with the transition high glass temperature. This means that when there is subjection to hot and dry air. The skin that results can overcome the coalescence of the droplets and interaction of sticky particles in the chamber used for dying (Jayasundera et al. [26]).

How conditions of spray drying process affect physicochemical, microstructural, and antioxidant properties of resulting fruit powder

The spray-dried fruit powder characteristics rely on the spray drying conditions such as the drying aid concentration, the temperature of the inlet, the rate of the feed flow, and the feed characteristics (Chegini et al. [17]). According to Nanda and Suhag, when they did their study on the spray drying process to produce lemon and orange fruit powder using the whey concentrate protein as a drying agent, the resulting process showed that when the air inlet temperature is increased, the bulk density is reduced, antioxidant activities are also reduced. However, there is an increase in the powder's hygroscope. When the concentrations of whey protein are increased, the bulk density increases while the powder hygroscope decreases. The increased whey protein concentration positively influences the activities of antioxidants and the vitamin C retention in the orange and lemon fruit powder produced. This shows the relationship between encapsulation superiority features of whey concentration protein and the prevention of damage caused due to oxidation.

Bandari and Fang (2012) also studied the spray drying process of orange fruit powder using orange fruit concentrates, whey protein isolate, and maltodextrin as drying agent materials. There was no recovery of fruit powder when the orange juice concentrates were spray-dried without spray drying agent materials. A protein of a small amount was efficient for the recovery of 50% powder for the orange fruit juice to be spray-dried, while maltodextrin in more significant amounts (around 30%) was required for the same purpose. There was a disclosure of the preferential protein migration to the droplet/particles surfaces by the authors, and the formation of a layer of glass during the process of spray drying resulted in the decreased adhesive property between the particles and the wall of the dryer during the fruit spray drying process of orange juice fruit concentrate. The ability of maltodextrin to reduce stickiness is because of the orange fruit powder's increased glass transition temperature. The authors who conducted the study reported that there was a low activity of water on the powder, about 5%, and the addition of whey protein at a percentage of 1 because whey protein has a level that has relation to the holding capacity of water in the protein. The graph below shows the relationship between moisture content and temperature in the process.

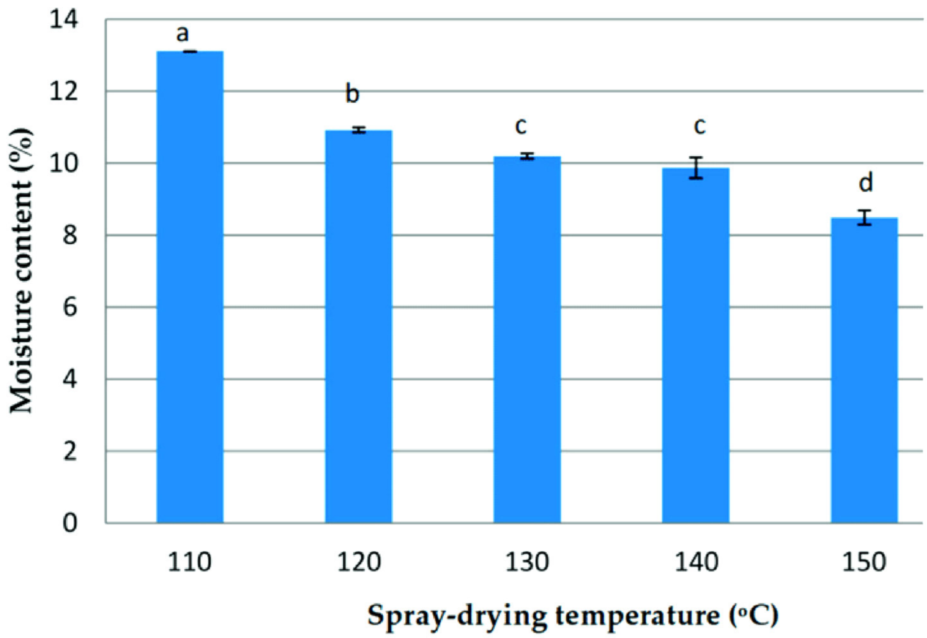

Figure 5.

Tonon et al. [15] researched the property of physicochemical in the spray drying of orange and lemon that is affected by the conditions of spray drying. The resulting solution showed that the yield in the powder production was influenced positively by the temperature of the inlet air. There was a negative influence on the feed flow rate related directly to the transfer of mass and heat. The addition of a concentrated form of drying agent (maltodextrin) reduced the yield of the process due to the higher viscosity of the feed solution. Flow rate and maltodextrin concentration had a favorable effect on the powder's water content, which was lowered due to increasing air temperature. The powder hygroscopic was reduced when maltodextrin content and feed flow rate were raised. According to powder morphology, the intake air temperature was also lowered. The higher inlet air temperature leads to a greater number of particles with smooth surfaces and big sizes due to the rapid drying rate of the drying agents utilized in this experiment.

Spray-dried orange juice powder's physicochemical properties were examined by Mishra et al. [16]; they used maltodextrin as a drying agent and inlet air temperature as a control. When the air input temperature and maltodextrin levels were varied, both water content and powder hygroscope were impacted. When maltodextrin content and the drying temperature are increased, the fruit powder loses some of its radical scavenging ability. The effect of drying rate and maltodextrin percentage on orange fruit powder's total phenolic content was shown.

Chegani et al. (2005) also conducted a study on the influence of the flow rate of the feed, the speed of atomization, and the air temperature of the inlet properties of the orange spray-dried powder. Results illustrate that an increase in the air inlet's temperature increased the particle's size; hence, the atomization speed increased.

Conclusion

The spray drying process is a technology that is important in producing fruit powder. Even though this technological process is good, it is associated with the problem of the stickiness of the powder juice that is occurring at a prevailing average temperature of the spray dryers. This problem is reduced by the use of the molecular weight of drying agents that is higher. The spray-dried fruit powder characteristics are influenced by the spray drying conditions, such as the drying agent material used, the temperature of the inlet, the rate of the feed flow, and the characteristics of the feed used. There are several ways of drying fruit powder. There is a way to dry them without using drying agents, and there is also drying by using a drying agent. There is also spray drying, which applies to oranges and lemons juice concentrates. It involves three steps: automation followed by droplet air contact, evaporation of moisture, and separation of dry products from exit air. In this method, spray drying affects the physicochemical, microstructural, and antioxidant properties of a fruit creating the fruit powder. When drying without using drying agents, water can act as a plasticizer and enhance the chaining of the irregular structure of the lemon and orange materials. The little water applied improves the reduction of the transition temperature of the glass until it reduces to temperatures below the home temperature. There are several types of fruit powders roller fruit powder, vacuum dried fruit powder, and freeze-dried fruit powder. All these forms have their advantages and disadvantages. For example, one disadvantage of freeze-drying, one requires water to complete the process. On the other hand, vacuum drying is advantageous because it can lengthen the storage time of the fruit powders while still maintaining the original flavor.

References:

1. Cabral A. C. S., Said S. and Oliveira W. P. Retention of the enzymatic activity and product properties during spray drying of pineapple stem extract in the presence of maltodextrin, International Journal of Food Properties, – 12. 2009. – P. 536–548.
2. Shrestha A. K., Ua-arak T., Adhikari B. R., Howes T. and Bhandari B. R. Glass transition behavior of spray-dried orange juice powder measured by differential scanning calorimetry (D. S. C.) and thermal-mechanical compression test (TMCT), International Journal of Food Properties, – 10. 2007. – P. 661–673.
3. Abadio F. D. B., Domingues A. M., Borges S. V., Oliveira V. M. Physical properties of powdered pineapple (Ananas comosus) juice – effect of malt dextrin concentration and atomization speed. J Food Eng – 64. 2004. – P. 285–287. URL: https://doi.org/10.1016/j.jfoodeng.2003.10.010
4. Adhikari B., Howes T., Shrestha A. K., Bhandari B. R. Development of stickiness of whey protein isolate and lactose droplets during convective drying. Chem Eng Process Process Intensif – 46. 2007. – P. 420–428. URL: https://doi.org/10.1016/j.cep.2006.07.014
5. Adhikari B., Drying Kinetics and Stickiness of Single Drop of Sugar and Acid-Rich Solutions. (Ph.D. thesis) Chemical Engineering. The University of Queensland, Australia, 2003.
6. Bhandari B. R., Senoussi A., Dumoulin E. D. and Lebert A. Spray drying of concentrated fruit juices, Drying Technology – 11. 1993. – P. 1081–1092.
7. Bhandari B. R., Data N. and Howes T. Problems associated with spray drying sugar-rich foods, Drying Technology, – 15. 1997. – P. 671–684.
8. Bae E. K., Lee S. J. Microencapsulation of avocado oil by spray drying using whey protein and maltodextrin. J Microencapsul – 25. 2008. – P. 549–560. URL: https://doi.org/10.1080/02652040802075682
9. Bazaria B., Kumar P. Effect of whey protein concentrate as drying aid and drying parameters on physicochemical and functional properties of spray dried beetroot juice concentrate. Food Biosci – 14. 2016. – P. 21–27. URL: https://sdoi.org/10.1016/j.fbio.2015.11.002
10. Bhandari B. R., Datta N., D'Arcy B. R., Rintoul G. B. Co-crystallization of honey with sucrose. LWT-Food Sci Technol – 31. 1998. – P. 138–142. URL: https://doi.org/10.1006/fstl.1997.0316

11. Bhusari S. N., Muzaffar K., Kumar P. Effect of carrier agents on physical and microstructural properties of spray dried tamarind pulp powder. Powder Technol – 266. 2014. – P. 354–364. URL: https://doi.org/10.1016/j.powtec.2014.06.038
12. Botrel D. A., de Barros Fernandes R. V., Borges S. V., Yoshida M. I. Influence of wall matrix systems on the properties of spray-dried microparticles containing fish oil. Food Res Int – 62. 2014. – P. 344–352. URL: https://doi.org/10.1016/j.foodres.2014.02.003
13. Cai Y. Z., Corke H. Production and properties of spray-dried amaranthus betacyanin pigments. J Food Sci – 65. 2000. – P. 1248–1252. URL: https://doi.org/10.1111/j.1365–2621.2000.tb10273.x
14. Cano-Chauca M., Stringheta P. C., Ramos A. M., Cal-Vidal J. Effect of the carriers on the microstructure of mango powder obtained by spray drying and its functional characterization. Innov Food Sci Emerg Technol – 6. 2005. – P. 420–428. URL: https://doi.org/10.1016/j.ifset.2005.05.003
15. Carneiro H. C. F., Tonon R. V., Grosso C. R. F., Hubinger M. D. Encapsulation efficiency and oxidative stability of flaxseed oil microencapsulated by spray drying using different combinations of wall materials. J Food Eng – 115. 2013. – P. 443–451. URL: https://doi.org/10.1016/j.jfoodeng.2012.03.033
16. Jing Du., Ge Z. Z., Xu Z., Zou B., Zhang Y. and Li C. M. Comparison of the Efficiency of Five Different Drying Carriers on the Spray Drying of Persimmon Pulp Powders, Drying Technology, – 32. 2014. – P. 1157–1166.
17. Emery E., Oliver J., Pugsley T., Sharma J., Zhou J. Flowability of moist pharmaceutical powders. Powder Technol – 189. 2009. – P. 409–415. URL: https://doi.org/10.1016/j.powtec.2008.06.017
18. Fang Z., Bhandari B. Comparing the efficiency of protein and maltodextrin on spray drying of bayberry juice. Food Res Int – 48. 2012. – P. 478–483. URL: https://doi.org/10.1016/j.foodres.2012.05.025
19. Frascareli E. C., Silva V. M., Tonon R. V., Hubinger M. D. Effect of process conditions on the microencapsulation of coffee oil by spray drying. Food Bioprod Process – 90. 2012. – P. 413–424. URL: https://doi.org/10.1016/j.fbp.2011.12.002
20. Fuchs M., Turchiuli C., Bohin M., Cuvelier M. E., Ordonnaud C., Peyrat-Maillard M. N., Dumoulin E. Encapsulation of oil in powder using spray drying and fluidized bed agglomeration. J Food Eng – 75. 2006. – P. 27–35. URL: https://doi.org/10.1016/j.jfoodeng.2005.03.047
21. Caliskan G. and Dirim S. N. The effects of the different drying conditions and the amounts of maltodextrin addition during spray drying of sumac extract, Food Bioproduct, and Processing, – 91. 2013. – P. 539–548.
22. Goula A. M., Adamopoulos K. G. A method for pomegranate seed application in food industries: seed oil encapsulation. Food Bioprod Process – 90. 2012. – P. 639–652. URL: https://doi.org/10.1016/j.fbp.2012.06.001
23. Sahin-Nadeem H., Dincer C., Torun M., Topuz A. and Ozdemir F. Influence of inlet air temperature and carrier material on the production of instant soluble sage (Salvia fruticosa Miller) by spray drying, LWT – Food Science and Technology, – 52. 2013. – P. 31–38.
24. Idham Z., Muhamad II., Setapar M., Hamidah S., Sarmidi M. R. Effect of thermal processes on roselle anthocyanins encapsulated in different polymer matrices. J Food Process Preserv – 36. 2012. – P. 176–184. URL: https://doi.org/10.1111/j.1745–4549.2011.00572.x
25. Jangam S. V., Thorat B. N. Optimization of spray drying of ginger extract. Dry Technol – 28. 2010. – P. 1426–1434. URL: https://doi.org/10.1080/07373937.2010.482699
26. Jayasundera M., Adhikari B., Howes T., Aldred P. Surface protein coverage and its implications on spray-drying of model sugar-rich foods: solubility, powder production and characterization. Food Chem – 128. 2011. – P. 1003–1016. URL: https://doi.org/10.1016/j.foodchem.2011.04.006

27. Jinapong N., Suphantharika M., Jamnong P. Production of instant soymilk powders by ultrafiltration, spray drying and fluidized bed agglomeration. J Food Eng – 84. 2008. – P. 194–205. URL: https://doi.org/10.1016/j.jfoodeng.2007.04.032
28. Kato Y., Matsuda T. Effects of the glycoprotein sugar chains on the amino-carbonyl reaction of chicken and Japanese quail ovomucoids with glucose. Biosci Biotech Biochem – 60. 1996. – P. 1490–1491. URL: https://doi.org/10.1271/bbb.60.1490
29. Lipasek R. A., Ortiz J. C., Taylor L. S., Mauer L. J. Effects of anticaking agents and storage conditions on the moisture sorption, caking, and flowability of deliquescent ingredients. Food Res Int – 45. 2012. – P. 369–380. URL: https://doi.org/10.1016/j.foodres.2011.10.037
30. Listiohadi Y. D., Hourigan J. A., Sleigh R. W., Steele R. J. An exploration of the caking of lactose in whey and skim milk powders. Aust J Dairy Technol – 60. 2005. – 207 p.
31. Lumay G., Boschini F., Traina K., Bontempi S., Remy J. C., Cloots R., Vandewalle N. Measuring the flowing properties of powders and grains. Powder Technol – 224. 2012. – P. 19–27. URL: https://doi.org/10.1016/j.powtec.2012.02.015
32. Imtiaz-Ul-Islam M. D. and Langrish T. A. G. Comparing the crystallization of sucrose and lactose in spray dryers, Food Bioproduct and Processing – 87. 2009. – P. 87–95.
33. Rascon M. P., Beristain C. I., García H. S. and Salgado M. A. Carotenoid retention and storage stability of spray-dried encapsulated paprika oleoresin using gum Arabic and soy protein isolate as wall materials, LWT- Food Science and Technology, – 44. 2011.
34. Mahendran T. Physico-chemical properties and sensory characteristics of dehydrated guava concentrate: effect of drying method and maltodextrin concentration. Trop Agric Res Ext – 13. 2011. – P. 48–54. URL: https://doi.org/10.4038/tare.v13i2.3138
35. Boonyai P., Bhandari B. and Howes T. Stickiness measurement techniques for food powders: a review, Powder Technology, – 145. 2004. – 34–46.
36. Santhalakshmy S., Bosco S. J. D., Francis S. and Sabeena M. Effect of inlet temperature on physicochemical properties of spray-dried Jamun fruit juice powder, Powder Technology – 274. 2015. –P. 37–43.
37. Maa Y. F., Nguyen P. A., Sit K. and Hsu C. C. Spray-drying performance of a bench-top spray dryer for protein aerosol powder preparation, Biotechnology and Bioengineering – 60. 1998. – P. 301–309.

Section 6. Economics and managementy

https://doi.org/10.29013/ESR-22-5.6-59-64

Vanishvili Merab,
PhD in Economics, Professor,
Georgian Technical University
Kokashvili Nanuli,
PhD in Economics, Associate Professor
Gori State Teaching University
Sosanidze Maka,
PhD in Economics, Associate Professor
Gori State Teaching University

GENDER BUDGETING IN THE FIELD OF GEORGIAN HEALTH AND SOCIAL PROTECTION: ANALYSIS AND EVALUATION

Abstract. Based on the latest literary sources and rich factual material, the scientific article consistently discusses topical issues of financial theory and practice, gender budgeting in the healthcare and social protection of Georgia.

It has been established that the spheres of health care and social orientation have a high gender significance. At the same time, the study shows that the state budget programs of Georgia do not contain gender sensitivity.

It is substantiated that the goals set in the health and social protection programs of the state budget of Georgia, and the indicators of intermediate and final results require more specification in accordance with the principles of the program budgeting methodology in general, as well as taking into account additional gender aspects.

Keywords: gender budgeting, program budgeting, gender sensitivity, gender gap, gender impact, gender analysis.

1. Introduction

Gender plays an important role in the origin and spreading of certain diseases/pathologies, as well as in their treatment and well-being. This is due to biological differences between the sexes, as well as socio-economic and cultural factors that influence the behavior of women and men and their use of health services (Shanava & Vanishvili [2]; Shanava & Vanishvili [3]; Vanishvili, Lemonjava et al. [8]; Gechbaia et al. [7]).

In general, it can be said that women are better than men, aware of the state of their health and are more active in using health services. There are several reasons for this: a) a reproductive role; b) their "caring" role; c) their large proportion in the entire older population; D) Gender stereotypes (Vanishvili Merab et al. [10]).

In Europe, the health sector is predominantly male. Women occupy lower positions in the sector (eg nurses and midwives) and are a minority among senior professionals (doctors, dentists). Women are also underrepresented in leadership positions in the sector. In addition, due to the high involvement of women in the health sector, special attention should be paid to gender-sensitive education.

Gender analysis is of particular importance in the social sphere. It is believed that the integration of gender issues in social areas such as health and social care is associated with the availability of relevant skills and therefore, gender is more pronounced than, for example, in the private sector and agriculture, which are more related to opportunities. An analysis of government subsidies or other social spending shows that when, for example, spending on health and social welfare is cut, it makes a gender difference – the increased burden falls on households and mainly on women. This issue is closely related to gender budgeting (Vanishvili & Sreseli [9]).

Gender budgeting involves incorporating gender equality considerations into a country's budget process and reallocating budgetary resources to facilitate gender mainstreaming in all areas or sectors. Due to the complexity of gender budgeting, there is no universal approach to it. The approach used and the institutional structure are usually based on the characteristics of a particular country.

Due to the urgency of the problem, the purpose of our study is to analyze and evaluate gender budgeting in the field of healthcare and social security in Georgia.

2. Materials and Methods

Well-known methods have been developed to assess the value of gender equality in health and social care, such as: 1) One Health tool developed under the International Health Partnership, It also includes analysis, evaluation and financing of the health nutrition system with the use of different scenarios; 2) "Cost of social protection" ("Calculation of the minimum cost of social protection"), which evaluates the closure of different social programs, checks their similarity and validity in case of increasing the social program; 3) Reproductive Contraceptive Instrument (UNFPA).

The Beijing Platform for Action emphasized the importance of gender budgeting in the social sector. In particular, interested developing and developed countries have agreed that, on average, 20% of the official development assistance budget and 20% of the social programs of the state budget should take into account a gender vision (Nathalie Holvoet [11]).

When evaluating capital projects, the following five main stages of gender budgeting are distinguished: 1) Analysis of the situation of women, men, girls and boys in the relevant infrastructure sector; 2) Assessing the gender sensitivity of programs, legislation and past projects; 3) Evaluation of the implementation of gender-sensitive activities and project proposals at the expense of budget allocations; 4) Monitoring the distribution of allocated funds, as well as services provided to the relevant target groups; 5) Assess the impact of the respective infrastructure project and the changed situation compared to the first phase.

The following two methods for analyzing gender budgeting of infrastructure projects are known: 1) *Gender-Disaggregated Beneficiary Assessment:* data for this estimator can be obtained through relevant surveys, household interviews, focus group discussions, direct observation, case studies and other methods. The main questions to be explored should be divided into gender, geographic region, level of education, status of opportunity, and other relevant categories; 2) *Gender Expenditure Analysis:* This method involves evaluating relevant budgets and policies in a gender-responsive manner to assess the allocation of resources to boys/men and girls/women. The main point of this method is to understand what gender influences the funded project has.

3. Results and discussion

According to the National Statistical Office of Georgia, as of January 1, 2022, the population of Georgia is 3688.6 thousand people (48% men, 52% women) and has been increasing by an average of

0.04% annually over the past 5 years. Over the past decade, on average, more boys are born each year than girls, and therefore the sex ratio at birth (male/female) is 1.08, while at the same time, the average annual sex ratio at death (male/female) is 1.05. This means that the number of men both in terms of fertility and mortality during this period is higher than that of women (http://gender.geostat.ge/gender/index.php?action= Demography).

The coefficient of natural increase (per 1000 population) is –3.8 as of January 1, 2022, this indicator has been decreasing by an average of 20% annually since 2014, more precisely, the difference between births and deaths is decreasing and the ratio of this difference to the total population decreases with the number (natural increase rate). If we consider this indicator by regions of the country, then during 2021 in all regions, except for the municipality of Tbilisi, the Autonomous Republic of Adjara, Samtskhe-Javakheti and Kvemo Kartli, there was a negative difference between births and deaths (https://www.geostat.ge/ka/modules/categories/321/ bunebrivi-mateba).

The average age of the population increased in 2022 compared to 2002 for both men (from 33.9 to 36.1 years) and women (from 37.9 to 40.4 years), which led to an increase in the average the age of the population during this period for both sexes (from 36 to 38.3 years). In terms of life expectancy (life expectancy at birth (year) disaggregated by sex), at the end of 2021 this figure is 71.4 years for both sexes, of which 75.4 years for women and 67.5 years for men. However, this indicator for both sexes has slightly decreased over the past 5 years (for comparison: 72.7 years in 2016 and 71.4 years in 2021).

One of the most important gender indicators in the field of health and social protection is the level of infant mortality. According to the State Statistics Service, compared with 2016, infant mortality will decrease by a total of 94 units in 2021 (from 507 to 413) (http://gender.geostat.ge/gender/index.php?action=Demography). And the mortality rate for children under 5 years old (per 1000 live births) for both sexes is slightly reduced (from 10.7 to 10.0) (https://www.geostat.ge/ka/modules/categories/320/gardatsvaleba).

Gender-relevant are age coefficients that measure the population aged 0–14 years and 65 years and older for every 15–64 years, or show the number of children and elderly dependents of the working-age population, which reached 54.1 as of January 1, 2022. Among them, 31.2 is the load factor by the age of young people, 22.9 is the load factor by the age of the elderly. This number has been growing over the years. In general, both in the case of the elderly and children, the load rate in women is higher than in men. With individual children, the load factor is higher for men, and for older children, for women (https://www.geostat.ge/ka/modules/categories/41/mosakhleoba).

It is also important to observe a country's household statistics for gender analysis of a country's social background. According to the 2014 census, there are about 1.109.130 households in the country, the average household size (number of people living in it) is 3.3, and this figure is approximately equal for urban (3.3) and rural (3.4) settlements. At the same time, the number of single-member households in the country is quite large (193.874 for both sexes), of which 63% are single women and 37% are single men (http://census.ge/ge/results /census1/households).

In terms of employment and economic activity in general, the economically active population (activity rate) for women is significantly lower than for men (for example, 56% and 74%, respectively, in 2021). This is why women have lower unemployment and employment rates than men.

In this regard, it is also interesting to consider the average monthly nominal wages of employees by type of activity and gender. The average salary of both sexes in 2015 was 900.4 lari, and in 2020–1191.0 lari. The salary of men is on average 1.5 times higher than that of women (in 2020, 1.407.7 lari and 952.2 lari, respectively (https://www.geostat.ge/ka/modules/categories/683/dasakmeba-umushevroba).

In this regard, it is also interesting to consider the average monthly nominal wages of employees by type of activity and gender. The average salary of both sexes in 2015 was 900.4 lari, and in 2020–1191.0 lari. The salary of men is on average 1.5 times higher than that of women (1.407.7 lari and 952.2 lari, respectively, in 2020). The difference between salaries has slightly decreased compared to 2015. In areas such as "financial and insurance activities", "health and social services", "professional, scientific and technical activities", "public administration and defense; Mandatory social protection "The gender wage gap has widened over this period and is still significantly higher. These differences are narrowing in areas such as wholesale and retail trade, as well as real estate, administrative and support services, education, and more. For many years only in one sector "Electricity, gas, steam and air conditioning" women's wages were higher (by an average of 1.1 times) than men's (https://www.geostat.ge/ka/modules/categories/39/khelfasebi).

As of 2021, the total number of pension and social package recipients is 971.648, of whom 65% are women and 35% are men. The share of women and men is different between pensioners and recipients of social packages. 71% of the 745.001 people receiving the pension are women, while 63% of the 226.647 people receiving the social package are men.

It should also be noted that according to the Social Services Agency, for example, in 2019, on average, more than 70.000 people receive a monthly state pension supplement due to their permanent residence status in a high-mountainous settlement. There are approxi-mately twice as many women among these persons as men; And in the same mountain village, the number of recipients of additional payments to the social package with permanent residence status exceeds 13 thousand every month, of which about 60% are men and 40% are women (http://ssa.gov.ge/ index.php?lang_id=&sec_id=1444).

According to the Social Services Agency, on average, 56% of the recipients of the planned component of outpatient services are women and 44% are men. In total, in 2019, 588.551 patients and 685.182 cases of illness were registered as beneficiaries of the universal health program, and the amount of compensation amounted to about 132 million lari. Thus, the cost of one case of treatment will be on average 198 GEL for both sexes, and the cost of one patient will be 224 GEL. Although the number of female and male patients eligible for the program is roughly evenly distributed, during this period, the amount reimbursed per unit in the case of men is approximately 8–9% higher than the amount reimbursed for women in the department (http://ssa.gov.ge/index.php?lang_id=&sec_id=1454).

An analysis of the current health and social situation in Georgia shows that these areas are of gender importance. Therefore, when planning and budgeting government programs, it is necessary to take into account the current situation and current gender needs, as well as analysis of international experience and research for the implementation of effective and adapted policies for relevant population groups (Vanishvili, Katsadze et al. [5]).

Regarding the gender analysis of medical and social programs provided for by the state budget, it should be noted that the priority "Affordable, high-quality healthcare and social security" includes nine budget programs according to the state budgets for 2019 and 2020 and the attached materials. For this priority, due to the magnitude of the priority, we find a very small entry in terms of gender relevance in the priority description part, also only in the 2019 budget and the attached country key data and directions document for 2019–2022 (Vanishvili & Katsadze [8]).

As world experience shows, due to the high gender significance of the healthcare and social protection sphere, the information available on the priority should include a gender vision and make it understandable (Vanishvili & Lemonjava [6]; Vanishvili & Lemonjava [7]).

4. Conclusion

In summary, it can be noted that the healthcare and social services sectors are of great gender importance, however, the analysis of the submitted budget laws shows that the state budget programs of Georgia do not disclose gender sensitivity. Most programs and sub-programmes are not gender sensitive, several programs differ in their gender relevance, There are also some targets set in terms of gender, however these are mostly presented in the form of statistics and do not adequately reflect gender needs. The goals, milestones and outcomes set in the program need to be more specific, both in accordance with the principles of the program budgeting methodology in general, and taking into account additional gender aspects.

References:

1. Gechbaia B., Vanishvili M., & Mushkudiani Z. Segmentation of Georgian Population According to Financial Capabilities and Money Management Style. Representation of Azerbaijan International Diaspora Center in Georgia. SCSJAR. 2017. – P. 4–9.
2. Shanava Z., & Vanishvili M. Analysis And Evaluation Of Financial Education Of The Population In Georgia. International Journal of Innovative Technologies in Economy, – 4 (36). 2021 a. – P. 77–88. URL: https://doi.org/10.31435/rsglobal_ijite/30122021/7740
3. Shanava Z., & Vanishvili M. Financial Education Of The Nation: Challenges And Perspectives. International Journal of Social Science and Economic Research, 06(12 "December 2021"). 2021 b. – P. 4646–4672. URL: https://doi.org/10.46609/IJSSER.2021.v06i12.012
4. Vanishvili M., & Katsadze I. Bank Financing Of Green Economy: Review Of Modern Research. Scientific Collection «InterConf», 2021. – (95). With the Proceedings of the 2 Nd International Scientific and Practical Conference «Scientific Goals and Purposes in XXI Century» (January 19–20, 2022). Seattle, USA: ProQuest LLC, 2022. – № 95 | January, 2022. – P. 120–143. URL: https://doi.org/10.51582/interconf.19–20.01.2022.
5. Vanishvili M., Katsadze I., & Vanishvili N. Public Finance Reform And State Transfer Policy In Georgia. Theoretical and Empirical Scientific Research: Concept and Trends: Collection of Scientific Papers «ΛΌΓΟΣ» with Proceedings of the II International Scientific and Practical Conference. – Vol. 1. Oxford, May 28, 2021. Oxford-Vinnytsia: P. C. Publishing House & European Scientific Platform, – 1. 2021. – P. 26–30. URL: https://doi.org/DOI 10.36074/logos-28.05.2021.v1
6. Vanishvili M., & Lemonjava L. Public Financial Management System in Modern Georgia. Refereed and Peer-Reviewed International Scientific-Practical Journal "Globalization & Business," – 6. 2016. –P. 129–133.
7. Vanishvili M., & Lemonjava L. Modern Budget Class ification in the Public Finance System of Georgia. Globalization & Business, – 12. 2017. – P. 47–50. URL: https://doi.org/DOI: 10.35945/gb
8. Vanishvili M., Lemonjava L., Katsadze I., & Vanishvili N. Loan Liabilities And Debt Burden Of The Population In Georgia. Grundlagen Der Modernen Wissenschaftlichen Forschung Der Sammlung Wissenschaftlicher Arbeiten «ΛΌΓΟΣ» Zu Den Materialien Der I Internationalen Wissenschaftlich-Praktischen Konferenz, Zürich, 10. September, 2021. Zürich-Vinnytsia: BOLESWA Publishers & Europäische Wissenschaftsplattform, – 1. 2021. – P. 29–35. URL: https://doi.org/DOI 10.36074/logos-10.09.2021
9. Vanishvili M., & Sreseli L. Challenges Of Gender Municipal Budgeting In Georgia. Scientific Collection «InterConf», (97): With the Proceedings of the 9 Th International Scientific and Practical Conference «International Forum: Problems and Scientific Solutions» (February 6–8, 2022). Melbourne, Australia: CSIRO Publishing House, 2022. – 612 p. – № 97 | February, 2022. – P. 108–112.
10. Vanishvili Merab, Kokashvili Nanuli, & Osadze Lali. The Saving Culture And Financial Goals Of Population In Georgia. European Science Review, – 9–10. 2021. – P. 35–40.

11. Nathalie Holvoet. Gender budgeting: its usefulness in the context of programme-based approaches: briefing note. European Commission. 2006. URL: https://www.researchgate.net/publication/282858691_Gender_budgeting_its_usefulness_in_the_context_of_programmebased_approaches_briefing_note
12. Gender Statistics. – URL: http://gender.geostat.ge/gender/index.php? action= Demography/ (Access date 19.06.2022).
13. Natural Increase. – URL: https://www.geostat.ge/ka/modules/categories/ 321/bunebrivi-mateba/ (Access date 19.06.2022).
14. DEATH – URL: https://www.geostat.ge/ka/modules/categories/320/gardatsva-leba/ (Access date 19.06.2022).
15. 2014 General Population Census. – URL: http://census.ge/ge/results/ census1/households/ (Access date 19.06.2022).
16. Employment And Unemployment. – URL: https://www.geostat.ge/ka/ modules/categories/683/dasakmeba-umushevroba/ (Access date 19.06.2022).
17. Saiaries. – URL: https://www.geostat.ge/ka/modules/categories/39/khelfasebi/ (Access date 19.06.2022).
18. Social Service Agency / Social package – from September 1. 2012 to 2019. – URL: http://ssa.gov.ge/index.php?lang_id=&sec_id=1444/ (Access date 19.06.2022).
19. Social Service Agency / Statistics on state programs for universal health care 2019. – URL: http://ssa.gov.ge/index.php?lang_id=&sec_id=1454/ (Access date 19.06.2022).

Contents

Section 1. Materials Science. 3

Nadareishvili Malkhaz, Kiziria Evgeni, Sokhadze Victor,
Tvauri Genadi, Gogichaishvili Shota, Jeremy Ramsden
PULSED DIFFERENTIAL CALORIMETRY OF THE HEAT CAPACITY JUMP AT
DENATURATION OF COLLAGEN TYPE I OF RAT TAIL TENDONS 3

Section 2. Medical science 11

Jiemuratova Gulparshin Koshkinbayevna, Kalandarova Amina Nurullayevna,
Kadyrova Aigul Amirbekovna
THE INFLUENCE OF ENVIRONMENTAL FACTORS ON THE NONSPECIFIC
IMMUNITY OF CHILDREN LIVING IN THE ARAL SEA REGION 11

Jiemuratova G. K., Danilova E.A., Akhmedjanova Z. I.
FEATURES OF CHANGES IN SOME MICROELEMENTS IN CHILDREN
OF THE ARAL SEA REGION 16

Section 3. Pedagogy 21

Terzieva Galena Todorova
ADAPTATION OF MOBILE GAMES FOR CHILDREN WITH
HEARING IMPAIRMENTS 21

Section 4. Physics 25

Daliev Shakhrukh Kh., Ergashev Javokhir A.
DEEP LEVEL TRANSIENT SPECTROSCOPY OF DEFECTS
IN SILICON MULTILAYER STRUCTURES DOPED WITH HAFNIUM ATOMS 25

Mahliyoxon Adxamovna Mamatova, Rasulov Rustam Yavkachovich,
Mirzaakbarov Dilshodbek, Kasimov Forrukh
RELATION BETWEEN THE CONCENTRATION OF NONEQUILIBRIUM
ELECTRONS AND HOLES IN LONG SEMICONDUCTOR DIODES 29

Rasulov Voxob Rustamovich, Rasulov Rustam Yavkachovich,
Mamatova Mahliyo Adhamovna, Khudoyberdiyeva Muhayyoxon Zoirjon-kizi,
Mamadaliyeva Nargiza Zokirjon-kizi
INFLUENCE OF A STRONG ELECTRIC FIELD ON THE CURRENT-VOLTAGE
CHARACTERISTIC OF THREE-LAYER SEMICONDUCTOR STRUCTURES IN
A DIODE CONNECTION 33

Rasulov Vohob Rustamovich, Rasulov Rustam Yavkachovich,
Mamatova Muhhayyo Adhamovna, Karimova Mahliyo Nematjon qizi,
Mirzaakbarov Dilshodjon Dovlatboyevich
VOLT-AMPERE CHARACTERISTICS OF A THREE-LAYER SEMICONDUCTOR
DIODE OF DOUBLE INJECTION 37

Utamuradova Sharifa Bekmuradovna, Naurzalieva Elmira Mahambetyarovna
RAMAN SPECTROSCOPY OF STRUCTURAL DEFECTS RELATED WITH
SILVER ATOMS IN SILICON 42

Section 5. Chemistry 46

Bulutoglu Efe
SPRAY DRIED FRUIT POWDER USING
FRUIT JUICE CONCENTRATES 46

Section 6. Economics and managementy 59

Vanishvili Merab, Kokashvili Nanuli, Sosanidze Maka
GENDER BUDGETING IN THE FIELD OF GEORGIAN HEALTH AND SOCIAL
PROTECTION: ANALYSIS AND EVALUATION 59